DIRICHLET DOMAINS FOR THE MOSTOW LATTICES

MARTIN DERAUX

Abstract. We describe an experimental method for studying the combinatorics of Dirichlet domains in the complex hyperbolic plane, based on numerical and graphical techniques.

We apply our techniques to the complex reflection groups that appear in Mostow's seminal paper on the subject, and list a number of corrections to the combinatorics of the Dirichlet domains.

1. Introduction

Very few explicit fundamental domains for lattices acting on spaces of non-constant curvature have been worked out, the main difficulty being the non-existence of totally geodesic hypersurfaces. There is of course a general construction, due to Dirichlet, but in concrete examples the combinatorics of such domains remain elusive.

In this paper we study this problem in the simplest symmetric space of non-constant negative curvature, namely the complex hyperbolic plane. It is a Hermitian symmetric space, and its study involves a beautiful interplay between ideas from hyperbolic geometry and complex analysis. It is also a particularly interesting space to consider because it is known that, at least in dimension up to three, the isometry groups of complex hyperbolic spaces are not super-rigid. Indeed, non-arithmetic lattices were first constructed by Mostow in [Mos80], and the list was expanded in [DM86] and [Mos86].

Mostow's original approach was to construct explicit fundamental domains for a certain class of groups generated by complex reflections (see section 2.3). The corresponding Dirichlet domains and their combinatorics turn out to be extremely difficult to analyze, especially with the computer technology available in the late 1970's. In fact, using the techniques of this paper on a modern computer, it becomes relatively easy to see that some of the domains in [Mos80] are incorrect (we explain the main difficulties in section 11). We point out that Mostow's main results, giving a criterion for discreteness and arithmeticity (see section 2.5), remain correct. Indeed, a number of proofs have appeared

Date: August 20, 2005.

in the literature, see [DM86] or [Thu98] for instance. However, the proof in [Mos80] has a serious gap.

We find it worthwhile to list the known mistakes in [Mos80], as an illustration of the possible pitfalls of experimental methods in this area of mathematics. More importantly, we give detailed techniques for testing claims about the combinatorics of Dirichlet domains. For the sake of concreteness, we shall focus mainly on Mostow's examples of lattices, but our techniques clearly apply to any group given by a set of generators. Another application of our experimental methods will be presented in a subsequent paper, see [Der05].

The use of computers is crucial throughout the analysis, and we shall not attempt to make our claims independent of the computer (even though it could quite reasonably be done). The latter was a recurrent theme in [Mos80], but it now seems somewhat artificial, the use of computers being much more widely accepted. Note that an intricate combination of numerical analysis and formal computations is needed in order to justify our experimental results rigorously, and we do not concentrate on that aspect in the present paper.

In order to prove discreteness rigorously, Dirichlet domains seem too rigid to be convenient. Many discreteness results proved to this day rely on the construction of polyhedra bounded by other kinds of hypersurfaces, avoiding the use of bisectors (see [Sch01], [FK02] for instance). However, Dirichlet domains provide an important tool during the first encounter with a given complex hyperbolic group. On the one hand, if the group is not discrete, our techniques usually produce an explicit sequence that accumulates to the identity (the powers of an elliptic element of infinite order). On the other, assuming that the group is indeed discrete, the conjectural Dirichlet domain points to key geometric features of the group - it suggests a way to find important conjugacy classes (by finding the stabilizers of the various faces), and to determine whether or not the quotient has finite volume (see [Der05]).

In the case of the Mostow lattices, the information gathered from the Dirichlet construction can be used quite naturally to build slightly simpler fundamental domains, and to prove discreteness using the Poincaré polyhedron theorem (see [DFP05]). Other fundamental polyhedra in the complex hyperbolic plane, not obtained by the Dirichlet construction, have been worked out in [FP05] and [Par05]).

Finally, we mention that our experimental methods give invaluable insight into the very intricate properties of bisector intersections, as studied already in [Gol99] (see also [Phi92] and [GP92]).

Acknowledgements: The author wishes to thank Elisha Falbel, John Parker, Julien Paupert, Anna Pratoussevitch, Richard Schwartz

and Pierre Will for many useful dicussions on the subject, as well as the referees for their useful comments and suggestions.

2. Complex hyperbolic geometry

It is a difficult problem to construct lattices in the isometry groups of symmetric spaces without using arithmetics. In spaces of constant curvature, a fairly simple class of groups is provided by reflection groups (i.e. groups generated by reflections). If the group is discrete, then the symmetric space is tiled by the connected components of the complement of the union of the mirrors of reflections in the group, each such component giving a fundamental domain for the action.

In complex hyperbolic space, the situation is much more complicated, since there is no good analogue of the faces of the above polyhedra: there are no real totally geodesic hypersurfaces. There are many isometric involutions that can play the role of reflections, but their fixed point sets have real codimension at least two, hence their complement is connected.

2.1. **The complex hyperbolic plane.** We review some basic material on the complex hyperbolic plane (for more details, we refer the reader to [Eps87] or [Gol99]). Consider a Hermitian form $\langle \cdot, \cdot \rangle$ of signature $(2,1)$ on $\mathbb{C}^3$, linear in the second variable and anti-linear in the second. We write H for its matrix in the standard basis $\{e_j\}$, so that $H_{ij} = \langle e_i, e_j \rangle$. We refer to a vector v as being positive, null or negative depending on the sign of the inner product $\langle v, v \rangle$.

The group of linear isometries preserving H is a non-compact group isomorphic to $U(2,1)$, and we consider its action on $P^2_{\mathbb{C}}$, the set of complex lines in $\mathbb{C}^3$. The group acting effectively is then $PU(2,1)$, and it acts transitively on the set of negative lines, i.e. the set of complex lines spanned be vectors v with $\langle v, v \rangle < 0$, with the stabilizer of a given line isomorphic to $U(2)$.

As a set, the complex hyperbolic plane $H^2_{\mathbb{C}}$ is the set of lines in $\mathbb{C}^3$ negative with respect to the Hermitian form (by the last paragraph, it is a homogeneous space $PU(2,1)/U(2)$). There is a natural metric, unique up to scaling, that makes the action of $PU(2,1)$ isometric. Endowed with such a metric, $H^2_{\mathbb{C}}$ becomes a symmetric space of $\frac{1}{4}$-pinched negative sectional curvature.

It is clear that the spaces obtained from different matrices H of signature $(2,1)$ are naturally isometric (up to scaling of the metric). In an orthonormal basis, the Hermitian form can be described as

$$\langle v, w \rangle = -v_0 \overline{w}_0 + v_1 \overline{w}_1 + v_2 \overline{w}_2 \tag{2.1}$$

Denoting by (x_0, x_1, x_2) the corresponding homogeneous coordinates, $H^2_{\mathbb{C}}$ is contained in the affine chart $x_0 \neq 0$, and in the coordinates $y_j = x_j/x_0$, it is simply given by the unit ball

$$|y_1|^2 + |y_2|^2 < 1$$

The Hermitian form (2.1) is called standard. It is convenient however to allow for non-standard coordinates, as we often do in this paper.

For the metric with curvature between -1 and $-1/4$, the distance between two points is given by the formula

$$\cosh(\frac{1}{2}d(x,y)) = \frac{|\langle x, y\rangle|}{\sqrt{\langle x, x\rangle\langle y, y\rangle}} \tag{2.2}$$

Here and in what follows, with a slight abuse of notation, we denote by the same symbol a vector in $\mathbb{C}^3$ and the complex line that it spans (note that the right hand side of the above formula does not change under scaling of the vectors).

2.2. **Totally geodesic subspaces.** Given a positive vector v, its orthogonal complement $v^\perp$ (with respect to H) is a 2-dimensional subspace on which the Hermitian form restricts to a form with signature $(1, 1)$. The set of negative lines in $v^\perp$ is then a copy of $H^1_{\mathbb{C}}$, naturally isometric to the Poincaré disk. It is easily seen to be totally geodesic, for instance by exhibiting it as the fixed point set of an isometry (in fact there is a 1-parameter family of isometries fixing it, see (2.3)).

Definition 2.1. The submanifolds of $H^2_{\mathbb{C}}$ given by $v^\perp$ are called **complex geodesics**. The vector v is called **polar** to the complex geodesic $v^\perp$.

Here we abuse notation once again, denoting by $v^\perp$ the set of negative lines in $\mathbb{C}^3$ spanned by vectors orthogonal to v with respect to H. Let ζ be any complex number of absolute value 1, and consider the linear map

$$R_{v,\zeta} : x \mapsto x + (\zeta - 1)\frac{\langle x, v\rangle}{\langle v, v\rangle}v \tag{2.3}$$

It is easy to check that these do indeed preserve the Hermitian inner product, that they fix the vectors in $v^\perp$, and that v gets multiplied by ζ. Geometrically, $R_{v,\zeta}$ fixes $v^\perp$ and rotates about it by the angle given by the argument of ζ.

Definition 2.2. The transformation $R_{v,\zeta}$ is called a complex reflection, with mirror $v^\perp$.

It is apparent from the formula (2.3) that the reflection remains unchanged under scaling of the vector v. In particular, we may assume that $\langle v, v\rangle = 1$ (in what follows we will always use this normalization).

Observe also that we may compose the above linear transformation by multiplication by a fixed scalar, without changing the corresponding isometry (scalar matrices act as the identity on projective space). A complex reflection is an isometry that can be lifted to a linear transformation of the form (2.3).

Another type of totally geodesic subspace is given in the standard ball model as the set of points with real coordinates, which is the fixed point set of the isometry $(y_1, y_2) \mapsto (\overline{y}_1, \overline{y}_2)$. In general for a non-necessarily standard Hermitian form, one gets such a subspace by taking three independent vectors v_1, v_2, v_3 with $\langle v_i, v_j\rangle \in \mathbb{R}$ for any i, j. The restriction of the Hermitian form to the real span of these vectors is then a quadratic form of signature $(2, 1)$, and the image in projective space of the set of negative vectors in the real span is simply a copy of $H^2_{\mathbb{R}}$. There is a unique isometry that fixes it, given in the basis of the v_j by

$$\sum \lambda_j v_j \mapsto \sum \overline{\lambda}_j v_j \tag{2.4}$$

Such a subspace is called *totally real* totally geodesic subspaces, or simply a *Lagrangian*.

It is a fact that all totally geodesic submanifolds of $H^2_{\mathbb{C}}$ are points, real geodesics, complex geodesics or Lagrangians (for a sketch of proof, see [Gol99]). It can also be checked that the above two types of submanifolds realize the extrema of sectional curvature (the complex geodesics being four times more curved than the totally real planes).

Finally we mention that $PU(2, 1)$ is the group of *holomorphic* isometries of $H^2_{\mathbb{C}}$, and has index two in the full group $\widehat{PU}(2, 1)$ of isometries. The latter is generated by $PU(2, 1)$ and one antiholomorphic involution as in (2.4).

2.3. **Complex reflection groups.** A natural way to describe a reflection group is to give a Coxeter diagram, having one node for each generator, and joining two nodes to mean that these generators should satisfy some braid relation (see [Cox67]).

The main difference with the real hyperbolic case is that such a diagram does not determine the group uniquely - there is one degree of freedom attached to each loop in the diagram (the so-called phase shift). A slightly more general discussion of Coxeter diagrams is given in [Mos80] - here we simply review Mostow's examples, given by the

following diagram (the meaning of the phase shift φ will be explained below).

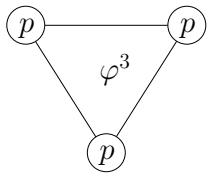

Here there are three generators of order p that satisfy the braid relation

$$R_i R_j R_i = R_j R_i R_j$$

We leave it to the reader to verify the following important result:

Proposition 2.3. *Let $R_1 = R_{v_1,\zeta_1}$ and $R_2 = R_{v_2,\zeta_2}$ be distinct complex reflections as in (2.3). Then $R_1R_2R_1 = R_2R_1R_2$ if and only if $\zeta_1 = \zeta_2$ and*

$$\frac{|\langle v_1, v_2\rangle|}{\sqrt{\langle v_1, v_1\rangle\langle v_2, v_2\rangle}} = \frac{1}{|\zeta_j - 1|} \tag{2.5}$$

Note that the left hand side of (2.5) is the cosine of the angle between the mirrors $v_1^\perp$ and $v_2^\perp$. In case $\zeta = e^{2\pi i/p}$, the right hand side can be written as

$$\frac{1}{2\sin\frac{\pi}{p}} \tag{2.6}$$

One sees that there is a one parameter family of possible configurations of mirrors of the generators, by the following rough dimension count: the space of triples of vectors has dimension twelve, the group $PU(2,1)$ has dimension eight, so the configuration space of polar vectors has dimension four. The braiding of the generators imposes the three angles between the mirrors of the generators, so we get only one free parameter. More precisely:

Proposition 2.4. *The space of configurations of triples of (distinct) braiding complex reflections of order p, up to conjugation by an element of $PU(2,1)$, is an interval.*

Proof: Let $R_j = R_{v_j,\zeta}$ (where $\zeta = e^{2\pi i/p}$) be the three braiding reflections. By scaling the vectors v_j, we may assume that $\langle v_i, v_i\rangle = 1$.

The braiding imposes $|\langle v_i, v_j\rangle|$, but we are still free to choose the argument of $\langle v_i, v_j\rangle$. By adjusting v_1 and v_3 (scaling them by a complex number of norm 1), we may assume that $\langle v_1, v_2\rangle = \langle v_2, v_3\rangle = 1$.

There is one parameter left, namely the argument of the complex number $\langle v_3, v_1\rangle$. Two configurations are equivalent under conjugation

by $PU(2,1)$ if and only if, after the above normalizations, we get the same argument for $\langle v_3, v_1\rangle$.

In particular, if the configurations are equivalent, then they have the same *Hermitian triple product*

$$\langle v_1, v_2\rangle\langle v_2, v_3\rangle\langle v_3, v_1\rangle$$

and it is easily checked that this is also a sufficient condition.

Definition 2.5. The quantity $\langle v_1, v_2\rangle\langle v_2, v_3\rangle\langle v_3, v_1\rangle$ is called the Hermitian triple product of v_1, v_2 and v_3, and it is denoted by $\langle v_1, v_2, v_3\rangle$.

A more symmetric way to normalize the inner products is to take $\langle v_1, v_2\rangle = \langle v_2, v_3\rangle = \langle v_3, v_1\rangle$. We then denote their common value by $-\alpha\varphi$, where $\alpha = 1/(2\sin\pi/p)$.

Definition 2.6. The complex number φ^3 such that $\langle v_1, v_2\rangle\langle v_2, v_3\rangle\langle v_3, v_1\rangle = -\alpha^3\varphi^3$ is called the **phase shift** of the configuration.

Since it is a complex number of norm 1, we refer to it only by its argument, and when it causes no confusion we call $\arg\varphi^3$ the phase shift as well.

It turns out that the phase shift cannot be chosen arbitrarily. To see this, let us first assume that the vectors v_j are linearly independent in $\mathbb{C}^3$. Consider the matrix of the Hermitian form in the basis $\{v_1, v_2, v_3\}$, normalized in a symmetric fashion as above:

$$H = \begin{bmatrix} 1 & -\alpha\varphi & -\alpha\overline{\varphi} \\ -\alpha\overline{\varphi} & 1 & -\alpha\varphi \\ -\alpha\varphi & -\alpha\overline{\varphi} & 1 \end{bmatrix} \tag{2.7}$$

There exists a configuration with phase shift φ if and only if H has signature $(2,1)$. In turn, this is equivalent to $\det(H) < 0$ (H is clearly not negative definite).

We have

$$\det(H) = 1 - 3\alpha^2 - \alpha^3(\varphi^3 + \overline{\varphi}^3)$$

which is negative for $\frac{1}{\pi}\arg(\varphi^3) \in]-t_0, t_0[$, where $t_0 = 3(\frac{1}{2} - \frac{1}{p})$.

The case where the vectors v_j are dependent is slightly more complicated. It can be seen that it corresponds to the endpoints of the above intervals, namely to $t = \pm t_0$.

Recall that we assume that the generators are distinct, so the span of any two vectors v_j is two-dimensional. We may choose v_1 and v_2 so that $\langle v_1, v_2\rangle = \alpha$, and take the third vector to be of the form $v_3 = \lambda(v_1 + \theta v_2)$ for $\lambda \in \mathbb{R}$ and $|\theta| = 1$. The braid relation can then be checked to impose $\lambda = 1$, and $\theta = i\eta$ or $\theta = -i\overline{\eta}$, where we write

$$\eta = e^{i\pi/p} \tag{2.8}$$

Then the triple Hermitian product $\langle v_1, v_2, v_3\rangle$ is checked to be either $\alpha^3 i\overline{\eta}^3$ or its complex conjugate $-\alpha^3 i\eta^3$ (to verify this, it is useful to note that $1/\alpha = -i(\eta - \overline{\eta})$). The last two values correspond to the phase shift at the points where $t = \pm t_0$.

Note that in this case the mirrors or the three generators all fix a common point, represented by a vector orthogonal to any two of the vectors v_j. □

In Mostow's notation, the group $\Gamma(p, t)$ is generated given by the above group with phase shift

$$\varphi^3 = e^{\pi i t}$$

We shall always assume that the phase shift satisfies the condition

$$|t| < 3(\frac{1}{2} - \frac{1}{p})$$

for the reasons stated in the proof of Proposition 2.4.

Moreover, in order to keep the notation as symmetric as possible, we shall use as homogeneous coordinates the ones given in the basis v_1, v_2, v_3 of vectors polar to the mirrors of the generating reflections. In particular, the Hermitian form is given by the matrix (2.7). Note also that in these coordinates, the symmetry of order three conjugating R_i into R_{i+1} (indices taken mod 3) is simply given by

$$J = \begin{bmatrix} 0 & 0 & 1 \\ 1 & 0 & 0 \\ 0 & 1 & 0 \end{bmatrix}$$

As above, we write $\eta = e^{\pi i/p}$, so that the reflections $R_j = R_{v_j,\eta^2}$.

The matrix of R_1 is given by

$$R_1 = \begin{bmatrix} \eta^2 & -\eta i\overline{\varphi} & -\eta i\varphi \\ 0 & 1 & 0 \\ 0 & 0 & 1 \end{bmatrix} \tag{2.9}$$

and the other generators are easily obtained, since $R_2 = JR_1J^{-1}$ and $R_3 = J^{-1}R_2J$.

2.4. **Finite groups.** Two of the generators R_i and R_j have common fixed point in the ball

$$\begin{aligned}
&\Leftrightarrow \quad \exists v \in e_i^{\perp} \cap e_j^{\perp},\ \langle v, v\rangle < 0 \\
&\Leftrightarrow \quad \mathrm{Span}_{\mathbb{C}}\{e_i, e_j\} \text{ is a positive definite subspace} \\
&\Leftrightarrow \quad \det \begin{bmatrix} \langle e_i, e_i\rangle & \langle e_i, e_j\rangle \\ \langle e_j, e_i\rangle & \langle e_j, e_j\rangle \end{bmatrix} < 0 \\
&\Leftrightarrow \quad |\langle e_i, e_j\rangle| < 1 \\
&\Leftrightarrow \quad p < 6
\end{aligned}$$

where in the last equivalence we have used the formula (2.6). Here we focus on the case $p < 6$, and denote by p_{ij} the point common to the mirrors of R_i and R_j (coordinates for that point are given in section 9).

If $p < 6$, the group Γ_{ij} generated by R_i and R_j can be seen as a subgroup of $U(2)$. A nice description of the group is obtained by studying its action on the complex projective line $P^1_{\mathbb{C}} \simeq S^2$ of complex lines through p_{ij} (in homogeneous coordinates this corresponds to the action on the positive definite subspace $p_{ij}^{\perp}$ of $\mathbb{C}^3$).

The generating reflections act as rotations by an angle $2\pi/p$, with centers at the vertices of an equilateral triangle with angles $2\pi/p$. These two spherical isometries are readily seen to generate the spherical triangle group $T_{2,3,p}$. For integers $p, q, r \geq 2$ with $1/p + 1/q + 1/r > 1$, we denote by $T_{p,q,r}$ the triangle group generated by rotations around the vertices of the spherical triangle with angles π/p, π/q and π/r. For $p = 3, 4$, or 5, $T_{2,3,p}$ is the group of orientation preserving autorphisms of the regular tetrahedron, cube or dodecahedron, which have order 12, 24, 60 respectively.

Finally, the group Γ_{ij} is a central extension of the triangle group $T_{2,3,p}$ (which is obtained by projectivization of the action on $p_{ij}^{\perp}$). The center of Γ_{ij} is generated by the appropriate power of R_iR_j, and has order 2, 4 and 10 in the cases $p = 3$, $p = 4$ and $p = 5$ respectively. In particular, Γ_{ij} has order 24, 96 or 600 for $p = 3$, 4 or 5 respectively.

We shall see in section 8 that the obvious relations (i.e. the order of the reflections and the braid relation) actually give a presentation for the finite group.

Finally we mention that the center of mass of the three mirrors of the generating reflections, which is also the center of mass of the fixed points p_{ij}, is given by the point

$$p_0 = [1, 1, 1]^T \tag{2.10}$$

Note that this is the isolated fixed point of the symmetry J.

p	$\lvert t\rvert < \frac{1}{2} - \frac{1}{p}$	$\lvert t\rvert = \frac{1}{2} - \frac{1}{p}$	$\lvert t\rvert > \frac{1}{2} - \frac{1}{p}$
3	$0, \mathbf{\frac{1}{30}}, \frac{1}{18}, \mathbf{\frac{1}{12}}, \mathbf{\frac{5}{42}}$	$\frac{1}{6}$	$\frac{7}{30}, \frac{1}{3}$
4	$0, \mathbf{\frac{1}{12}}, \mathbf{\frac{3}{20}}$	$\frac{1}{4}$	$\frac{5}{12}$
5	$\frac{1}{10}, \mathbf{\frac{1}{5}}$		$\frac{11}{30}, \frac{7}{10}$

TABLE 1. Pairs (p, t) for which the conditions of the Poincaré theorem hold. Numbers in boldface yield non-arithmetic lattices.

2.5. **Mostow's main results.** We review the two main results of [Mos80].

Theorem 2.7. *If* $(\frac{1}{4} - \frac{1}{2p} \pm \frac{t}{2})^{-1} \in \mathbb{Z} \cup \{\infty\}$*, then* $\Gamma(p, t)$ *is a lattice in* $PU(2, 1)$*.*

The above conditions come out naturally by studying the cycles of 2-faces of the Dirichlet domains, in the terminology of the Poincaré polyhedron theorem (see section 7). Indeed, certain cycle transformations are complex reflections that rotate around the appropriate 2-face by angles $2\pi(\frac{1}{4} - \frac{1}{2p} \pm \frac{t}{2})$ (see section 10).

There are only finitely many values of (p, t) that satisfy the condition in the theorem, given in Table 1. The condition of Theorem 2.7 is almost necessary for discreteness, and in fact it follows from the work in [Mos88] that there is only one more discrete group among the groups $\Gamma(p, t)$ with $p = 3$, 4 or 5, namely $\Gamma(5, \frac{1}{2})$. In that case the Dirichlet polyhedron can be divided as a union of fundamental domains by considering the finite group that fixes p_0 (we shall not discuss this issue).

One gets more groups (but still finitely many) by allowing $p > 5$ but for the sake of brevity, we shall not discuss this here (that issue and much more is treated in the various papers by Mostow and co-authors given in the bibliography, where the groups are described in terms of monodromy groups of hypergeometric functions). Some of the groups for $p > 5$ are also studied in [Par05].

As mentioned before, the lattices of the theorem are particularly interesting because of the following:

Theorem 2.8. *The lattices* $\Gamma(p, t)$ *are non-arithmetic for* $(p, t) = (3, \frac{1}{30})$*,* $(3, \frac{1}{12})$*,* $(3, \frac{5}{42})$*,* $(4, \frac{1}{12})$*,* $(4, \frac{3}{20})$ *or* $(5, \frac{1}{5})$*.*

For the definition of arithmeticity, see [Mos80], [DM86].

3. Dirichlet fundamental domains

Given any group Γ acting on $H^2_{\mathbb{C}}$, the Dirichlet domain centered at p_0 is by definition

$$F = \{x \in H^2_{\mathbb{C}} : d(x, p_0) \leq d(x, \gamma p_0),\ \forall \gamma \in \Gamma\} \tag{3.1}$$

The group Γ acts discretely if and only if F has non-empty interior, and in that case F is a fundamental domain for Γ, as long as no element of the group fixes the point p_0. If p_0 is fixed, then one only gets a fundamental domain modulo the action of the finite group that fixes it.

Note that F is bounded by a number of hypersurfaces of equidistance, also called bisectors. Even though their definition makes sense in any metric space, it is easy to imagine that these hypersurfaces could be quite pathological, in particular they need not be smooth or connected in general. Here we focus on the case of $H^2_{\mathbb{C}}$, where Dirichlet domains were already considered by Giraud in [Gir21], see also [Mos80] and [Gol99].

In practice, it is quite difficult to verify whether or not F is non-empty and, if so, to determine its combinatorics. It is not even clear whether it has finitely many faces (in fact this is not true in general, even for some very elementary groups, see [GP92]).

We wish to study cases where F only has finitely many faces, so that we can actually write the polyhedron as

$$F = F_W = \{x \in H^2_{\mathbb{C}} : d(x, p_0) \leq d(x, \gamma p_0),\ \forall \gamma \in W\} \tag{3.2}$$

for some finite subset $W \subset \Gamma$.

The main difficulties can be summarized as follows:

1. How do we find an appropriate set W?
2. Given a finite set $W \subset \Gamma$, how do we determine the combinatorics of F_W?
3. Does F_W have side pairings, and does it satisfy the cycle conditions of the Poincaré polyhedron theorem (see section 7)?

Part 1 is usually very tedious, but it can be done by computer experimentation (a detailed procedure is given in [Der05]).

For the Mostow groups, one easily obtains a guess for reasonable candidates for the sets W (but one needs to be very cautious, the guess taken in [Mos80] seems reasonable, but it is not always correct, as we shall discuss in section 11).

Part 2 is the most difficult. We shall describe experimental methods for doing this with a computer, but it turns out that it is extremely difficult to prove the results rigorously.

Assuming part 2 has been done correctly, part 3 is very straightforward (most of the verifications follow automatically from the fact that F_W is obtained by a Dirichlet construction).

4. Elementary properties of bisectors

Dirichlet polyhedra are bounded by hypersurfaces equidistant between two points in complex hyperbolic space. These are not totally geodesic, and can have fairly complicated intersection patterns. We review some of the results in [Mos80] and [Gol99].

Definition 4.1. The **bisector** between two distinct points p_0 and p_1 in $H^2_{\mathbb{C}}$ is the set of points that are equidistant from p_0 and p_1:

$$\mathcal{B}(p_0, p_1) = \{x \in H^2_{\mathbb{C}} : d(x, p_0) = d(x, p_1)\} \tag{4.1}$$

The formula for the distance between two points was given in equation (2.2). We shall always rescale the vectors p_j so that $\langle p_0, p_0\rangle = \langle p_1, p_1\rangle$, and the equation of the bisector then becomes simply

$$|\langle x, p_0\rangle| = |\langle x, p_1\rangle| \tag{4.2}$$

In order to get points inside complex hyperbolic space, we consider only negative vectors $x \in \mathbb{C}^3$, $\langle x, x\rangle < 0$. It is sometimes useful, however, to study the solution set in all of $\mathbb{C}^3$, or rather in projective space $P^2_{\mathbb{C}}$. The corresponding solution set is then (a special case of) an extor (see [Gol99] for the definition).

4.1. **Slice decomposition.** The solution set of the equation $|\langle x, p_0\rangle| = |\langle x, p_1\rangle|$ is obviously foliated by complex lines $\langle x, p_0\rangle = \mu\langle x, p_1\rangle$, for complex numbers μ with $|\mu| = 1$.

Equivalently, each solution in $\mathbb{C}^3$ is on a unique complex plane of the form $v_\mu^\perp$, where

$$v_\mu = p_0 - \mu p_1,\ |\mu| = 1 \tag{4.3}$$

Equation (4.3) parametrizes a circle σ, which splits into two arcs σ^- and σ^+, consisting of vectors of negative or positive norm, respectively.

The $v_\mu^\perp$, for $v_\mu \in \sigma^+$, yield a foliation of the bisector by complex geodesics in the ball, called the *slice decomposition*. It is easy to check that any complex geodesic contained in the bisector must be a leaf of that foliation.

For each vector v_μ, there is a unique vector v_ν that is orthogonal to it (it is clear that the only ν that works is given by $\nu = \langle p_0, p_0 - \mu p_1\rangle / \langle p_1, p_0 - \mu p_1\rangle$). In particular, the arc σ^- is itself contained in the bisector, and by construction it is contained in the complex geodesic Σ

spanned by p_0 and p_1. Now the intersection of Σ with $\mathcal{B}$ is obviously a real geodesic, equidistant between p_0 and p_1.

Definition 4.2. The geodesic σ^- is called the *spine* of the bisector. The complex geodesic spanned by p_0 and p_1, is called its *complex spine*.

With a little abuse of language, we sometimes refer to the whole circle σ as the spine, and to the complex projective line containing it as the complex spine. When this causes any confusion, we refer to them as extended (real or complex) spines.

It is clear from the above description that the slices of the bisector are orthogonal to its spine (and to its complex spine). This is how the slice decomposition is usually stated:

Proposition 4.3. *Every bisector is the inverse image of its real spine under orthogonal projection onto its complex spine. The fibers of the projection are called the complex slices of the bisector.*

Definition 4.4. A bisector $\mathcal{B}$ is equidistant from a point x if there is a point y such that $\mathcal{B} = \mathcal{B}(x, y)$.

We leave the following as an exercise to the reader.

Lemma 4.5. *Let $\mathcal{B}$ be a bisector with real spine σ and complex spine Σ. Then $\mathcal{B}$ is equidistant from x if and only if $x \in \Sigma \setminus \sigma$.*

There is another natural decomposition of bisectors, into totally real geodesic subspaces: such a subspace is contained in the bisector if and only if it contains its real spine. Following [Gol99], we shall call these totally real subspaces the *meridians* of the bisector.

4.2. **Ball coordinates.** The equation of a general bisector in ball coordinates is quadratic in the real and imaginary parts of the coordinates, as can easily be seen from (4.2).

Lemma 4.6. *The equation of any bisector $\mathcal{B}$ in ball coordinates is a polynomial of degree at most two in the real and imaginary parts of the coordinates. It is linear if and only if the origin of the coordinates lies on the real spine of $\mathcal{B}$.*

From the decomposition in meridians, the lemma follows from the well known fact that a Lagrangian is linear if and only if it contains the origin (think of the 1-dimensional analogue, saying that geodesics in the Poincaré disk are straight lines if and only if they go through the origin).

Hence, given a pair of bisectors, there is no system of coordinates where they both have a linear equation (unless their real spines intersect).

4.3. **Bisectors in Dirichlet domains.** In view of the discussion in section 4.2, in order to find the combinatorics of a Dirichlet domain, one must describe the solution set of a number of quadratic inequalities. We shall only consider the cases where we have a finite number of such inequalities. Our approach consists in reducing the problem to a 2-dimensional one, by determining the combinatorics of the various 2-faces of the domain separately. Such 2-faces lie on the intersection of two bisectors - we will describe a way to obtain convenient coordinates on the intersection in section 5.

The bisectors bounding a Dirichlet domain F_W (see section 3) form a very special family of bisectors, namely they are all equidistant from a given point p_0. In view of Lemma 4.5, this means that all their complex spines intersect (Goldman calls such bisectors co-equidistant, see [Gol99]).

Another important property is the following.

Lemma 4.7. *Let $\mathcal{B}_1$ and $\mathcal{B}_2$ be two coequidistant bisectors. Then $\mathcal{B}_1 \cap \mathcal{B}_2$ cannot contain any totally real totally geodesic subspace.*

Proof: Let $\mathcal{B}_j = \mathcal{B}(p_0, p_j)$. Suppose L is a totally real totally geodesic subspace in the intersection. Then it contains both real spines, hence the antiholomorphic involution in L preserves both bisectors, but would have to interchange p_0 and p_j, hence $p_1 = p_2$. □

The intersection of co-equidistant bisectors can certainly contain a complex geodesic, however.

Lemma 4.8. *Let $\mathcal{B}_1$ and $\mathcal{B}_2$ be two coequidistant bisectors, whose intersection contains a complex geodesic. Then their complex spines are equal, and their real spines intersect.*

Proof: The only complex geodesics contained in a bisector are its slices (see [Gol99]). Suppose the two bisectors contain a complex geodesic S. By the slice decomposition, S is orthogonal to both complex spines. Since the complex spines have a point in common, they must coincide (otherwise one would get a geodesic triangle whose angles add up to more than π). The fact that the real spines intersect follows immediately from the slice decomposition (see Proposition 4.3). □

The following result is crucial to the study of Dirichlet domains.

Theorem 4.9. *Let $\mathcal{B}_1$ and $\mathcal{B}_2$ be two co-equidistant bisectors with distinct complex spines. Then their intersection is a smooth non-totally geodesic disk, which is contained in precisely three bisectors.*

If $\mathcal{B}_j = \mathcal{B}(p_0, p_j)$, $j = 1, 2$, then the third bisector of the Proposition is of course $\mathcal{B}(p_1, p_2)$. The fact that there are no other bisector containing $\mathcal{B}_1 \cap \mathcal{B}_2$ is due to Giraud, and the fact that the intersection is connected was proved by Goldman (see [Gol99]).

Definition 4.10. The intersection of two co-equidistant bisectors with distinct complex spines is called a **Giraud disk**. We also say that the two bisectors have Giraud intersection.

We summarize the previous result as follows: the intersection of two co-equidistant bisectors, if non-empty, is either a complex totally geodesic disk or a Giraud disk.

As we shall see in the next section by exhibiting explicit coordinates, if the intersection is Giraud then the equations $|\langle x, p_0\rangle| = |\langle x, p_1\rangle| = |\langle x, p_2\rangle|$ define a *torus* in projective space, referred to as a Clifford torus in [Gol99]. We sometimes call it a Giraud torus, since it extends a Giraud disk. Note that it is the intersection in projective space of the two extors that extend the bisectors $\mathcal{B}_j$ (see [Gol99] for more on extors).

The following result refines the statement that bisectors in complex hyperbolic space are not totally geodesic (for a proof see [Mos80] or [Gol99]).

Lemma 4.11. *Let q_1 and q_2 be two distinct points on the bisector $\mathcal{B} = \mathcal{B}(p_0, p_1)$. The geodesic between q_1 and q_2 is contained in $\mathcal{B}$ if and only if these points are in some slice or meridian of $\mathcal{B}$.*

In fact Dirichlet domains, which are intersections of half spaces bounded by bisectors, are not convex (even though they are clearly star-shaped with respect to the center of the domain).

Definition 4.12. For $\gamma \in \Gamma$, we write $\widehat{\gamma}$ for the bisector

$$\widehat{\gamma} = \mathcal{B}(p_0, \gamma^{-1} p_0)$$

Remark 4.13. Note that we use the same definition as Mostow, in order to make it easier to compare with the original text [Mos80]. Most references mentioning Dirichlet domains would probably call this bisector $\widehat{\gamma^{-1}}$ instead.

It is obvious from the definition that α sends $\widehat{\alpha}$ to $\widehat{\alpha^{-1}}$, and more generally

$$\alpha(\widehat{\alpha} \cap \widehat{\beta}) = \widehat{\alpha^{-1}} \cap \widehat{\beta\alpha^{-1}} \tag{4.4}$$

Note that this relation becomes much more natural when naming the bisectors in the usual way, see Remark 4.13.

Consider a Dirichlet domain F_W as in (3.2). For a given $\gamma \in W$, note that $\widehat{\gamma} \cap F_W$ need not be a topological ball in general, see [Der05] for examples.

As a consequence, one needs to define faces carefully, namely by taking the open faces to be the *connected components* of the interior of $\widehat{\gamma} \cap F_W$ in $\widehat{\gamma}$.

With "faces" interpreted in that manner, one proves just as in Lemma 3.3.2 of [Mos80] that the faces are topological balls. Note however that Mostow's Lemma 3.3.1 (which claims that for any $\gamma \in W$, the intersection of any complex slice of the bisector $\widehat{\gamma}$ intersects F_W in a convex polygon) is incorrect.

5. Experimental methods

5.1. **Spinal coordinates on bisector intersections.**

5.1.1. *Cospinal bisectors.* The bisectors $\mathcal{B}(p_0, p_1)$ and $\mathcal{B}(p_0, p_2)$ have the same complex spine if and only if p_0, p_1 and p_2 are represented by linearly dependent vectors in $\mathbb{C}^3$.

It follows from the slice decomposition (see Proposition 4.3) that two cospinal bisectors intersect if and only if their two real spines intersect, in a point p. In that case, their intersection consists of a complex geodesic S, which is perpendicular to their common complex spine through p.

We then choose a basis $\{v_1, v_2\}$ for (the lift to $\mathbb{C}^3$ of) S, with $\langle v_1, v_2\rangle = 0$, $\langle v_1, v_1\rangle = -1$, and $\langle v_2, v_2\rangle = 1$, so that a nice coordinate on S is obtained by writing its vectors as $v_1 + zv_2$, $|z| < 1$. The intersection $S \cap \mathcal{B}(p_0, p_3)$ with a third bisector has an equation of the form

$$|\langle v_1 + zv_2, p_0\rangle| = |\langle v_1 + zv_2, p_3\rangle|$$

which is a (possibly degenerate) circle in the z-plane. In particular, the intersection of S with a number of half spaces is bounded by circles or lines in the plane, which we consider an easy problem (even though one needs to be careful with issues of precision). One should be aware however that such an intersection need not be connected in general, since the arcs of circles bounding it are not necessarily geodesics.

5.1.2. *Giraud disks.* We now explain a convenient way to parameterize Giraud intersections. Consider two coequidistant bisectors $\mathcal{B}(p_0, p_1)$ and $\mathcal{B}(p_0, p_2)$, which we assume not to be cospinal (i.e. the three points p_j are represented by linearly independent vectors in $\mathbb{C}^3$).

We de-homogenize the coordinates on the affine chart given by the complement of $p_0^\perp$. In other words we use $y = x/\langle x, p_0\rangle$ as coordinates, and these three coordinates satisfy $\langle y, p_0\rangle = 1$.

The bisector intersection is then given by

$$\begin{array}{l} |\langle y, p_1\rangle| = 1 \\ |\langle y, p_2\rangle| = 1 \end{array} \tag{5.1}$$

We simply take u_1, u_2 as complex coordinates on the ball, where $u_j = \langle y, p_j\rangle$, so that the Giraud disk is the intersection with the ball of the torus

$$|u_1| = |u_2| = 1 \tag{5.2}$$

in projective space. We refer to u_1 and u_2 as *spinal coordinates*.

Note that complex hyperbolic space will not be given by the unit ball in the coordinates (u_1, u_2). In fact the intersection of the torus with $H^2_{\mathbb{C}}$ can be obtained as follows. Let P be the matrix whose columns are the coordinates of the vectors p_j, so that we have

$$\begin{aligned} y^T H\overline{P} &= [1, u_1, u_2] = U^T \\ \langle y, y\rangle &= U^T (P^T H\overline{P})^{-1}\overline{U} \end{aligned}$$

The last expression can be rewritten in the form

$$a_0 + 2\mathfrak{Re}\{a_1 u_1 + (a_2 + a_3\overline{u}_1)u_2\}$$

where the a_j are easily obtained from the Hermitian matrix $(P^T H\overline{P})^{-1}$. Observe that a_0 is real (it comes from the diagonal entries of the Hermitian matrix $P^T H\overline{P}$), whereas the other a_j are in general complex.

The trace on the torus $|u_1| = |u_2| = 1$ of the boundary of the ball can obtained by solving a family of quadratic equations

$$\begin{cases} 2\mathfrak{Re}\{\alpha z\} = \beta \\ |z| = 1 \end{cases} \tag{5.3}$$

where

$$\begin{array}{l} \alpha = \alpha(u_1) = a_2 + a_3\overline{u}_1 \\ \beta = \beta(u_1) = -a_0 - 2\mathfrak{Re}\{a_1 u_1\} \end{array} \tag{5.4}$$

It is not obvious a priori than the intersection with the ball is connected, but this was proved by Goldman in [Gol99]. In other words, there is a unique arc on the circle $|u_1| = 1$ for which the equations (5.3) have a solution (and there are two solutions in the interior of the interval).

It is elementary to see that (5.3) has a solution if and only if

$$|\beta| \leq 2|\alpha| \tag{5.5}$$

In fact there is a unique solution if $|\beta| = 2|\alpha|$, two solutions if $|\beta| < 2|\alpha|$, and infinitely many if $\alpha = \beta = 0$.

In particular, the arc of values of u_1 where the trace of the unit ball projects can be obtained by solving the inequality

$$|a_0 + a_1 u_1 + \overline{a}_1 \overline{u}_1| < 2|a_2 + a_3 \overline{u}_1|$$

which can be rewritten as a degree four equation in the real or imaginary part of u_1. This immediately implies that there can be at most two connected components in the intersection of the bisectors, but coequidistance implies that there is only one (see [Gol99]).

It is clear from the description that the circles $u_1 = const$ correspond to the intersection of the slices of the first bisector with the second, and $u_2 = const$ to the intersection of the slices of the second bisector with the first bisector. The slices of the third bisector $\mathcal{B}(p_1, p_2)$ are easily seen to intersect the torus in "lines of slope one", namely $u_2 = \mu u_1$, $|\mu| = 1$.

Remark 5.1. The above three families of curves, given by the intersection with the ball of the horizontal, vertical and slope one slices of the Clifford torus, can be proved to be hypercycles in the Poincaré disk of the appropriate slice of the respective bisectors (see [Mos80] or section 7.3 of [Gol99]). We shall not need this fact in the present paper, all we need is the fact that they are arcs of circles.

5.2. **Exploring the 2-faces.** In order to understand the combinatorics of intersections of half-spaces bounded by bisectors, we want to study all of its 2-faces separately. Given the intersection S of two given bisectors, we want to determine the intersection of S with a number of half spaces bounded by finitely many other bisectors.

Our strategy is to plot on S the trace of all the other bisectors, and to consider the connected components of the complement of the union of these curves. We shall give some explicit examples in section 6, but for now we start with some general considerations. We focus on the case where S is a Giraud disk, the cospinal case being much easier to handle (see section 5.1.1).

Using spinal coordinates u_1 and u_2 on $S = \mathcal{B}(p_0, p_1) \cap \mathcal{B}(p_0, p_2)$, we write the equation of another bisector $\mathcal{B}(p_0, p_3)$ as

$$|\delta_0 + \delta_1 u_1 + \delta_2 u_2| = 1 \tag{5.6}$$

The coefficients δ_j are obtained as follows. Remembering that we normalize our coordinates so that $\langle y, p_0 \rangle = 1$, the coefficients δ_j are simply defined by the relation

$$p_3 = \overline{\delta}_0 p_0 + \overline{\delta}_1 p_1 + \overline{\delta}_2 p_2 \tag{5.7}$$

This makes sense because we assumed that the vectors p_0, p_1 and p_2 are independent and have the same norm. Note that there is some

ambiguity since we could multiply p_1, p_2 or p_3 by complex numbers of absolute value one, but this simply results in shifting the coordinates u_j by multiplication by a complex number of absolute value one.

Along each slice where u_1 is constant, the corresponding values of u_2 are obtained by solving equations exactly as in (5.3), now with

$$\begin{aligned} \alpha &= \overline{(\delta_0 + \delta_1 u_1)}\delta_2 \\ \beta &= 1 - |\delta_0 + \delta_1 u_1|^2 - |\delta_2|^2 \end{aligned} \tag{5.8}$$

Once again, for a given u_1, such an equation has 0, 1, 2 or infinitely many solutions.

Away from the degenerate cases, one obtains an explicit parameterization for the intersection $S \cap \mathcal{B}(p_0, p_3)$, of the form

$$u_2 = \frac{\beta \pm \sqrt{\beta^2 - 4|\alpha|^2}}{2\alpha} \tag{5.9}$$

with α and β depending on u_1 as in (5.8). This parameterization is only valid on the locus of $|u_1| = 1$ where the discriminant $\Delta = \beta^2 - 4|\alpha|^2$ in (5.9) is strictly negative (which could consist of up to two arcs on the circle).

The locus where $\Delta > 0$ is irrelevant, and the behavior of the curve $S \cap \mathcal{B}(p_0, p_3)$ on the locus $\Delta = 0$ is readily analyzed (there is either a unique solution for u_2, or u_2 is arbitrary). In the next section, we shall describe one possible computer program that plots these curves, for instance by using log coordinates t_j where $u_j = e^{2\pi i t_j}$. The only difficulty is to handle the degenerate situations – note that the only problem with our parameterization is the presence of "vertical lines" in the graphs. The cases where u_2 is arbitrary for a given value of u_1 are easy to detect in equation (5.6). They correspond to having either $\delta_2 = 0$, or $|\delta_2| = 1$ and $u_1 = -\delta_0/\delta_1$ (a geometric interpretation of these two cases is given in [Der05]).

Remark 5.2.

(1) There is of course a similar parameterization corresponding to solving for u_1 in terms of u_2. This gives another way to handle the vertical lines that could possibly appear in the u_1-parameterization. It is easy to understand when there are horizontal or vertical lines on the graph in terms of the coefficients δ_j of (5.6).

(2) Consider a case where a vertical line occurs at some u_1, but there are two distinct values of u_2 for nearby values of u_1. It can be checked (see [Der05]) that the parameterizations (5.9) have a limit on both sides, so that dividing by numbers close to 0 does not cause too much trouble in the results.

5.3. **Description of a computer program.** The java applet [Der] provides a convenient way to explore the combinatorics of the 2-faces of Dirichlet domains for the Mostow groups (or for any group given by an explicit set of generators). From there one can deduce the combinatorics of the whole Dirichlet domain, at least conjecturally.

There are of course two cases, depending on whether the 2-face is totally geodesic or not. This is done by computing the determinant of $P = [p_0, p_1, p_2]$, and if the determinant is close to zero, we shall consider the bisectors as being cospinal (in [Der] we use double precision, and consider the bisectors cospinal if $|detP|^2 < 10^{-10}$).

If the bisectors are (at least close to being) cospinal, we draw a number of circles on the unit disk, which is an easy task – we shall not worry about issues of precision here, and consequently we give no claim of rigor in the combinatorics of our Dirichlet domain.

If the bisectors have Giraud intersection, we use spinal coordinates, and produce a plot in log coordinates - recall we write $u_j = e^{2\pi i t_j}$. In our program [Der], we split the interval of values of $t_1 \in [a, b]$ into 500 equal pieces, and for each value of t_1 in the grid, we check whether $\Delta(u_1) \geq 0.0$ and, if it is, we use expression (5.9) to plot the corresponding two points on the graph.

The main problem with the above is that we might be missing some vertical lines in the graph. The simplest way to handle this (which is implemented in [Der]) is to plot the graph a second time, using u_2 as the parameter instead of u_1.

Figure 1 shows five curves traced on a torus (identified with a square with real coordinates t_1 and t_2, so that $u_j = e^{2\pi i t_j}$). The picture was drawn using Maple, for greater precision than in [Der] (in fact the pictures obtained by both methods are practically identical). The thick oval is the intersection with the boundary of the ball, the interior of the ball corresponding to the interior of the oval. The other curves correspond to intersections with four bisectors, two of them having two irreducible components.

6. Dirichlet domains for the finite groups

Recall from section 2.4 that the groups $\Gamma(p, t)$ contain natural finite subgroups Γ_{ij}, generated by R_i and R_j. For convenience of notation, we consider the group Γ_{12} (the other ones are obtained by conjugation by the isometry J).

Natural fundamental domains can be obtained from the description in terms of triangle groups given in section 2.4, by lifting the sides of the triangle on $\mathbb{P}^1_{\mathbb{C}}$ to totally real planes in $H^2_{\mathbb{C}}$ (this is the approach

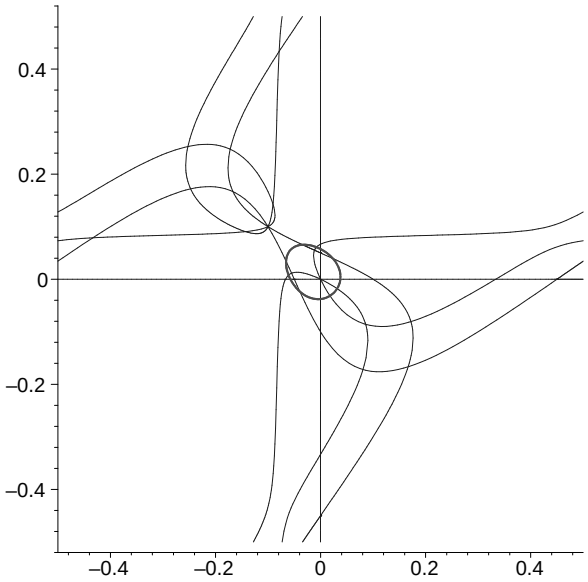

FIGURE 1. The trace of four bisectors on some generic bisector intersection

taken in [FP04]). Such domains will not be Dirichlet domains, however. In fact we will see that the Dirichlet domains for Γ_{12} are much more complicated, and in particular, they are far from being cones over the fixed point p_{12}.

Indeed, recall that the equation for a bisector in non-homogeneous ball coordinates is in general a quadratic equation in the real and imaginary parts of the coordinates (see section 4.2). The equation reduces to a linear one if and only if the real spine of the bisector goes through the origin of the system of non-homogeneous coordinates.

In particular, if we center the coordinates at the fixed point p_{12}, and take a point $p_0 \neq p_{12}$, none of the bisectors bounding the Dirichlet domain centered at p_0 will be linear! This explains the perhaps unexpected complexity of the results of this section. We mention that the results stated here differ quite significantly from the claims in [Mos80].

Specifically, Mostow claims that for any p, t, the fundamental domain F_{12} has only 10 faces (which sounds surprising since the groups Γ_{ij} have very different orders for different values of p). The specific set W_{12} of group elements that Mostow uses is

$$W_{12} = \{R_i^{\pm 1}, (R_i R_j)^{\pm 1}, (R_i R_j R_i)^{\pm 1}, i \neq j = 1, 2\}$$

Recall that the generating reflections braid, i.e. $R_1 R_2 R_1 = R_2 R_1 R_2$ (see section 2), so that the above set really consists of only 10 elements, and not 12, as might appear at first sight.

Once again, this might sound surprising since the order of Γ_{ij} changes when p changes. Note also that it is unclear whether or not the set of relevant words should be the same when t changes (the groups Γ_{ij} for various values of t are of course isomorphic, but the position of the mirrors of generating reflections with respect to the center of the Dirichlet domain changes).

Proposition 6.1. *For $p = 3$, the polyhedron F_{12} has at least 18 faces, and the group elements of the form $(R_iR_jR_i^{-1})^{\pm 1}$ and $R_iR_j^{-1}$ **need** to be included in order to obtain a fundamental domain.*

The conjectural combinatorics of F_{12}, for small phase shift, i.e. $|t| < \frac{1}{2} - \frac{1}{p}$, are given in Figures 6 and 7 (compare with the pictures on p.220 of [Mos80]). Note that the precise combinatorics are conjectural, even though the fact that a certain face is non-empty can easily be proved rigorously. We only list the case $p = 3$ and small phase shift for the sake of brevity, and because we are interested not so much in the finite groups but rather in the corresponding lattices.

Our pictures are obtained using the experimental method sketched in section 5, without worrying about the dependence on the phase shift parameter (we fix a particular set of braiding reflections by fixing a value of the phase shift φ).

6.1. **Examples of 2-faces.** We now describe some examples of $\widehat{\alpha_1} \cap \widehat{\alpha_2} \cap F_{12}$, where F_{12} is the Dirichlet domain for the finite group Γ_{12}, centered at the barycenter of the mirrors of the three reflections R_1, R_2 and R_3, namely $p_0 = [1, 1, 1]^T$.

These sets can be fairly complicated, and in particular it is not clear whether or not they are connected.

Definition 6.2. The connected components of the set ${}^*(\widehat{\alpha_1} \cap \widehat{\alpha_2}) =$

$$\{x \in \widehat{\alpha_1} \cap \widehat{\alpha_2} : d(x, p_0) < d(x, \gamma p_0),\ \forall \gamma \in \Gamma_{12}, \gamma \neq 1, \alpha_1^{-1}, \alpha_2^{-1}\} \tag{6.1}$$

are called are called *open 2-faces* of the polyhedron F_{12}.

It turns out that all the sets (6.1) in the Dirichlet domains for the groups that appear in [Mos80] are connected, so we shall not bother giving different names to the connected components. Note that in general however these sets are not connected (for examples, see [Der05]).

As we shall see in the examples below, the closure of that open 2-face is not necessarily equal to

$$\widehat{\alpha_1} \cap \widehat{\alpha_2} \cap F_{12} = \{x \in \widehat{\alpha_1} \cap \widehat{\alpha_2} : d(x, p_0) \leq d(x, \gamma p_0),\ \forall \gamma \in \Gamma_{12}\} \tag{6.2}$$

which can have lower-dimensional components.

6.1.1. *A cospinal example:* We start with the easier case, where the two bisectors $\widehat{\alpha_1}$ and $\widehat{\alpha_2}$ are cospinal (in which case their intersection is simply a complex line L). Recall that this is equivalent to saying that p_0, $p_1 = \alpha_1^{-1} p_0$ and $p_2 = \alpha_2^{-1} p_0$ are linearly dependent.

Recall from the discussion in section 5 that the intersection of a bisector $\widehat{\gamma}$ with the complex line L is an arc of a circle (except for degenerate situations, where L is a complex slice of $\widehat{\gamma}$). Once again we mention that it can be proved that this arc is actually a hypercycle (see Remark 5.1 and [Gol99]).

We discuss the example $\widehat{R_1} \cap \widehat{R_1^{-1}}$ in some detail. Since R_1 is a complex reflection, this intersection is simply the mirror of R_1. The corresponding 2-face $\widehat{R_1} \cap \widehat{R_1^{-1}} \cap F_{12}$ is a sector bounded by two geodesics for small phase shift, and it is slightly more complicated for large phase shift (see Figures 2 and 3).

The point p_{12} is fixed by the whole group Γ_{12}, so that all the corresponding bisectors go through a given point, which we take to be the origin of the disk coordinates.

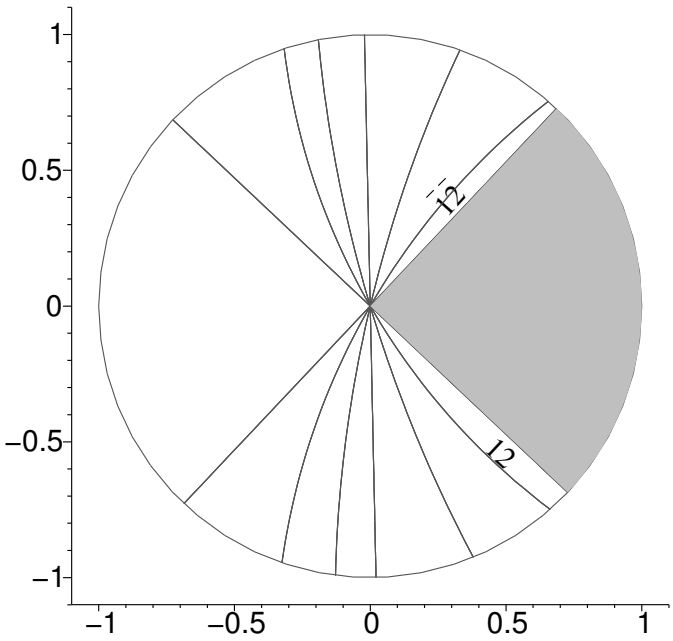

FIGURE 2. The 2-face of F_{12} on the mirror of R_1, for $p = 3$ and $t = 1/18$

Remark 6.3. The pictures given here can be obtained with the applet [Der], but the reader should be aware that the notation for bisectors

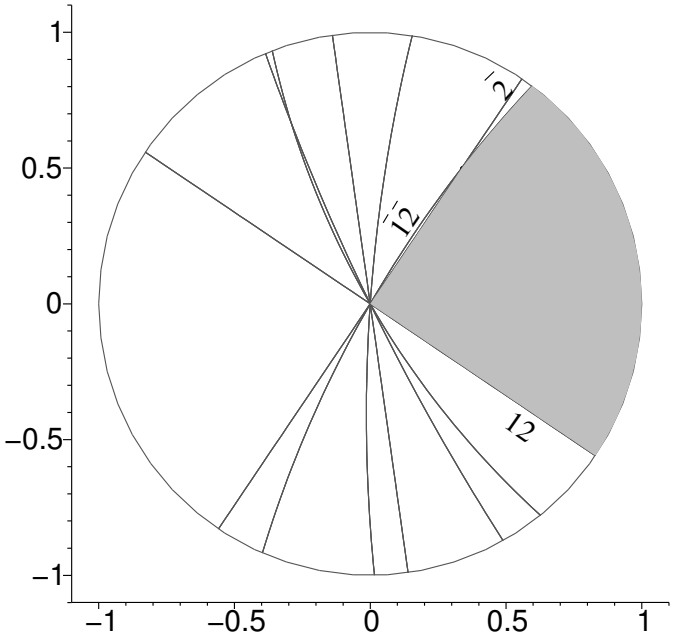

FIGURE 3. The 2-face of F_{12} on the mirror of R_1, for $p = 3$ and $t = 11/30$.

is opposite from the one used in the present paper (see Remark 4.13). In the applet, $\widehat{\gamma}$ stands for $\mathcal{B}(p_0, \gamma p_0)$ rather than $\mathcal{B}(p_0, \gamma^{-1} p_0)$.

6.1.2. *2-faces on Giraud disks.* If p_0, $p_1 = \alpha_1^{-1} p_0$ and $p_2 = \alpha_2^{-1} p_0$ are linearly independent, then the intersection $\widehat{\alpha_1} \cap \widehat{\alpha_2}$ is not totally geodesic but, as discussed in section 4, it has natural coordinates and we can easily plot the various intersections $\widehat{\alpha_1} \cap \widehat{\alpha_2} \cap F_{12}$ using a computer.

We discuss a couple of examples of 2-faces that illustrate the main difficulties. The shaded region in Figure 4 is the open 2-face ${}^*(\widehat{R_1} \cap \widehat{R_1 R_2 R_1})$. In order to obtain such a picture, we start by plotting all intersections with $\widehat{\gamma}$ in spinal coordinates u_1, u_2 (in the picture we actually use t_1 and t_2 where $u_j = e^{2\pi i t_j}$). This cuts the disk $\widehat{R_1} \cap \widehat{R_1 R_2 R_1}$ into a number of regions, and it is a bit tedious but not particularly difficult to test which ones are in the intersection of all the appropriate half-spaces γ^+.

One striking point is that $\widehat{R_1} \cap \widehat{R_1 R_2 R_1} \cap F_{12}$ consists of the closure of the open face ${}^*(\widehat{R_1} \cap \widehat{R_1 R_2 R_1})$, *together with an edge*. Indeed, the whole ray from the origin down along the vertical axis in the picture is contained in F_{12}, which is in fact contained in the intersection of the five bisectors corresponding to R_1, R_1^{-1}, $R_1 R_2$, $R_1 R_2 R_1$ and $R_1 R_2 R_1^{-1}$.

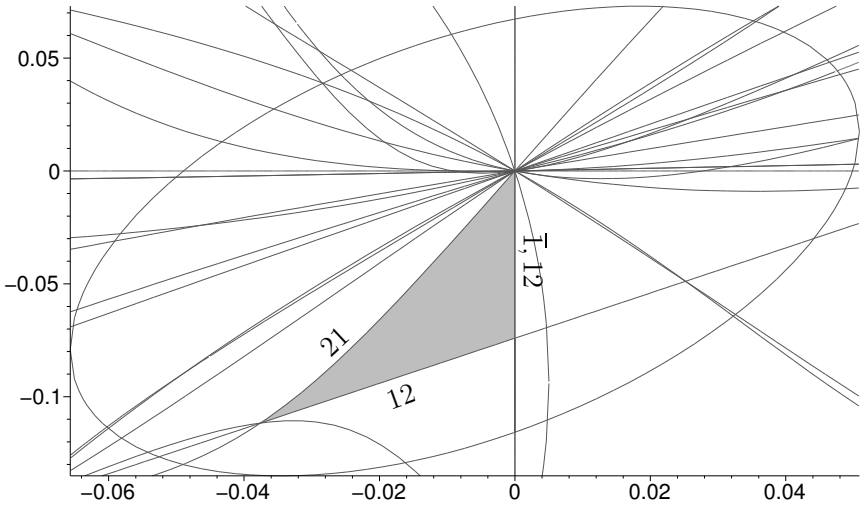

FIGURE 4. The open 2-face ${}^*(\widehat{R_1} \cap \widehat{R_1R_2R_1})$ for $p = 3$, $t = 1/18$.

This should be only partly surprising, since we already analyzed the intersection of these bisectors in $\widehat{R_1} \cap \widehat{R_1^{-1}} = e_1^{\perp}$, and found that it was indeed a ray that goes all the way to the boundary of the ball (see Figure 2).

We draw one more neighboring face, namely ${}^*(\widehat{R_1} \cap \widehat{R_1R_2})$. Once

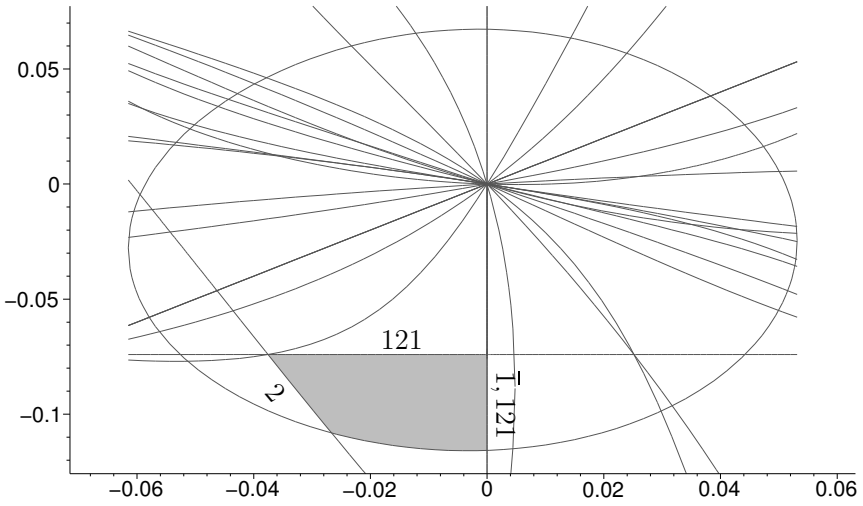

FIGURE 5. The open 2-face ${}^*(\widehat{R_1} \cap \widehat{R_1R_2})$ for $p = 3$, $t = 1/18$.

again, $\widehat{R_1} \cap \widehat{R_1R_2} \cap F_{12}$ contains a segment that is not in the closure of the open face (but that is actually part of the closure of the previous open face ${}^*(\widehat{R_1} \cap \widehat{R_1R_2R_1})$).

6.2. **Description of all the 2-faces.** It is quite clear that the methods from the previous paragraph allow one to describe all the possible 2-faces of the fundamental domain, by repeating the above procedure for all possible pairs of bisectors $\widehat{\alpha_1} \cap \widehat{\alpha_2}$ in the group (or rather in a well chosen finite set of elements in the group). In this manner, one gets a proof of Proposition 6.1.

There are of course issues of precision, and we do not attempt to prove the results rigorously. The main point is that it is fairly easy to prove that a given 2-face is non-empty, but it is tedious to prove that the precise combinatorics are as they seem from experimentation.

Figures 6 and 7 describe the results for $p = 3$ and $t = 1/18$. It is not clear that the same combinatorics hold for any small phase shift, i.e. whenever $-(\frac{1}{2} - \frac{1}{p}) < t < (\frac{1}{2} - \frac{1}{p})$, or for different values of p. In fact one can see (cf. section 11) that, for $p = 5$, the combinatorics are not stable on the intervals corresponding to large phase shift, $|t| > \frac{1}{2} - \frac{1}{p}$.

For the sake of saving space, we only show some faces that are representative of all the combinatorial possibilities. It is easy to deduce the combinatorics of the other faces by symmetry (see section 8).

Finally we mention that these figures correct the pictures given on page 220 of [Mos80], and that the domains are not cones over the point p_{12}.

7. The Poincaré polyhedron theorem

The most convenient way to transform our experimental results into rigorous proofs would be to use the appropriate version of the Poincaré polyhedron theorem.

Let $F = F_W$ be the polyhedron in $H^2_{\mathbb{C}}$ bounded by the bisectors $\hat{w} = \mathcal{B}(p_0, w^{-1}p_0)$, $w \in W$. Suppose W is symmetric (i.e. $w^{-1} \in W$ whenever $w \in W$), and w yields a side pairing transformation

$$w : F \cap \hat{w} \to F \cap \widehat{w^{-1}} \tag{7.1}$$

so that the image of the polyhedron F under the side pairing w intersects F along one face precisely, with no further intersection.

In what follows we shall sometimes write $\widetilde{w}$ for the face of F on the bisector $\hat{w}$, i.e.

$$\widetilde{w} = F \cap \hat{w} \tag{7.2}$$

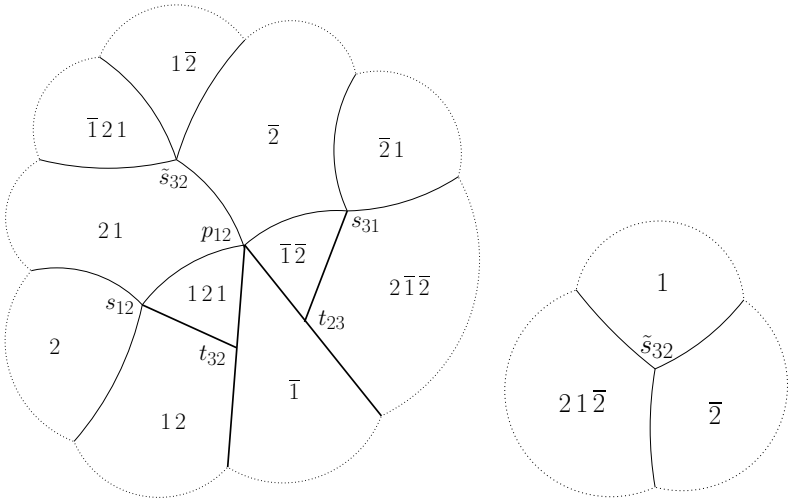

(a) $\widetilde{R_1}$ (b) $\widetilde{R_1 R_2^{-1}}$

FIGURE 6. The combinatorics of some faces of F_{12}, for small phase shift ($t = 1/18$). On each 2-face, we write a shortcut notation for the neighboring face $\widehat{\gamma}$, using i and $\overline{i}$ for R_i and R_i^{-1} respectively.

although the notation is somewhat ambiguous since $\tilde{w}$ depends on the poolyhedron F.

Since the side pairing w sends $\widetilde{w}$ to $\widetilde{w^{-1}}$, we write this condition as

$$F \cap w(F) = \widetilde{w^{-1}} \tag{7.3}$$

The following construction gives the cycle tranformation attached to each codimension two face, usually refered to as "edges". Let e_0 be such an edge. It is contained in the intersection $\widetilde{v_0} \cap \widetilde{w_0}$ of two faces for a unique choice of $v_0, w_0 \in W$. Consider the image of the edge under the side pairing corresponding to one of these two transformations, say v_0. Since it is a codimension two face of F, we can write it as

$$e_1 = v_0(e_0) = \widetilde{v_1} \cap \widetilde{w_1}$$

for some group elements $v_1, w_1 \in W$. Note that one of these two, say w_1, is simply v_0^{-1}.

Consider the image of e_1 under v_1, and write

$$e_2 = v_1(e_1) = \widetilde{v_2} \cap \widetilde{w_2} \tag{7.4}$$

for $w_2 = v_1^{-1}$ and v_2 uniquely determined by equation (7.4). Repeat this process to define a sequence of group elements v_k, w_k, $k = 1, \ldots, r+1$,

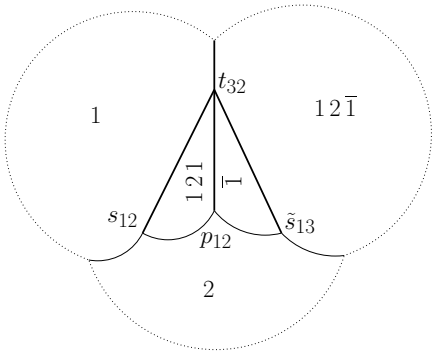

(a) $\widetilde{R_1R_2}$

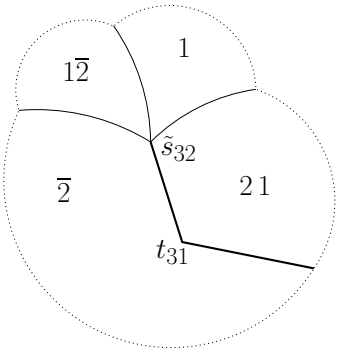

(b) $\widetilde{R_2R_1R_2^{-1}}$

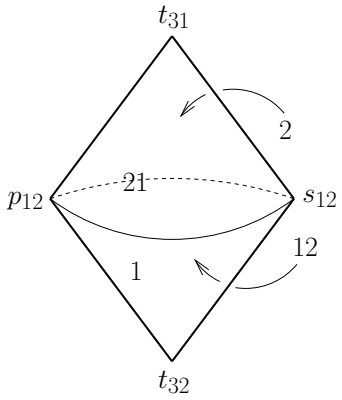

(c) $\widetilde{R_1R_2R_1}$

FIGURE 7. The combinatorics some faces of F_{12}, for small phase shift ($t = 1/18$). The dotted lines are contained in the boundary of the ball, whereas the dashed ones have a different meaning. One edge is dashed in (c) simply to indicate that it is hidden behind another 2-face.

until the first time we come back to the edge we started with, i.e.

$$e_{r+1} = e_0 \tag{7.5}$$

Note that we are certain that this process terminates since our set W is finite.

Definition 7.1. The group element $g_0 = v_r v_{r-1} \dots v_1 v_0$ is called the **cycle transformation** associated to the edge $e_0 = \widetilde{v_0} \cap \widetilde{w_0}$.

Here we require that g_0 be the identity on e_0 (i.e. this is part of the requirement (7.5)).

The element g_0 is not quite well defined, in fact it depends on the choice we made for the first side pairing (we could have chosen w_1 instead of v_1). It is readily checked that the other choice would simply yield the inverse cycle g_0^{-1}.

Let g_e denote the cycle transformation associated to the edge e of F. Suppose that for each edge e, the cycle g_e has finite order r_e and the successive images of F under the transformation g_e tile a neighborhood of the edge e, overlapping only along faces of the images of F (in particular the interiors of the images of F should be disjoint).

Theorem 7.2. *Under the above assumptions, the group Γ generated by W in $PU(2,1)$ is discrete, and F is a fundamental domain for Γ modulo the action of the finite subgroup of Γ that fixes p_0.*

If no element of Γ fixes p_0, a presentation for Γ is given by

$$\langle W | g_e^{r_e} = 1 \rangle \tag{7.6}$$

where the g_e are the words defining the cycle transformations as in Definition 7.1.

A proof of this result is sketched in [Mos80], see also [FP05]. Note that the fact that our faces are not totally geodesic complicates matters quite a bit, not only in proving the theorem but also in verifying whether its hypotheses are satisfied. It is very difficult to prove that two given polyhedra (bounded by bisectors, which are not totally geodesic) intersect precisely along one of their faces, even though, as we mentioned before, it can easily be tested experimentally.

We mention that Giraud's result (Theorem 4.9) is a very useful tool for verifying (7.1). Indeed, it implies that most of the edges (here we regard totally geodesic edges as being exceptional) are contained in precisely three bisectors, of which only two are equidistant from the center of our Dirichlet domain. Indeed, suppose $e = \widetilde{\alpha} \cap \widetilde{\beta}$ is a generic edge (i.e. the coequidistant bisectors $\widetilde{\alpha}$ and $\widetilde{\beta}$ are not cospinal, or in other words p_0, $p_1 = \alpha^{-1}p_0$ and $p_2 = \beta^{-1}p_0$ are not on a common complex line).

Then e is on precisely three bisectors, namely $\mathcal{B}(p_0, p_1)$, $\mathcal{B}(p_0, p_2)$ and $\mathcal{B}(p_1, p_2)$. Now $\alpha(e)$ is also a generic edge, and it is equidistant from $\alpha(p_0)$, $\alpha(p_1) = p_0$ and $\alpha(p_2) = \alpha\beta^{-1}(p_0)$.

As long as none of the group elements α, β, $\beta\alpha^{-1}$ fixes p_0, this means we know precisely what group elements we need to take in order to obtain the cycle transformation, there will be three such transformations and their product will be the identity.

We emphasize one implication of the above discussion: if a generic face $\widetilde{\alpha} \cap \widetilde{\beta}$ appears in the polyhedron F, then the face $\widetilde{\alpha^{-1}} \cap \widetilde{\beta\alpha^{-1}}$ must appear as well (provided that none of these group elements fixes p_0). In particular, this gives a necessary condition for the polyhedron F_W corresponding to a set W of group elements to have side pairings, which we refer to as being Giraud-closed:

Definition 7.3. We say that the set W is Giraud-closed if whenever $\alpha, \beta \in W$ and the open two-face of F_W in $\widehat{\alpha} \cap \widehat{\beta}$ is generic and non-empty, we have $\beta\alpha^{-1} \in W$.

This also gives a procedure for finding an appropriate set W, by including more and more group elements if necessary until W becomes Giraud-closed (but this procedure might never terminate). For more details on this, see [Der05].

If W is indeed Giraud-closed (this is difficult to verify rigourously), then the verification of the hypotheses of the Poincaré polyhedron theorem is reduced to verifications about complex geodesic 2-faces, which is much easier (the corresponding cycle transformations are then complex reflections, and one simply needs to study their angles of rotation).

8. Symmetries in the fundamental domain

8.1. **Basic symmetry.** The basic symmetry in the fundamental domain comes from the fact that the map

$$\begin{bmatrix} x_1 \\ x_2 \\ x_3 \end{bmatrix} \mapsto \begin{bmatrix} \overline{x_2} \\ \overline{x_1} \\ \overline{x_3} \end{bmatrix} \tag{8.1}$$

is an (antiholomorphic) isometry of complex hyperbolic space. It is readily checked that it conjugates R_1 into R_2^{-1} and R_2 into R_1^{-1}. This shows that we only need to consider half of the faces of the fundamental domain.

As in section 7, we write $\widetilde{\gamma}$ for the face $F_{12} \cap \widehat{\gamma}$ on the bisector γ. Now for any $\gamma \in \Gamma_{12}$, the isometry γ takes the face $\widetilde{\gamma}$ isometrically into $\widetilde{\gamma^{-1}}$. Once we have the combinatorics of $\widetilde{R_1}$, we can deduce the combinatorics of $\widetilde{R_1^{-1}}$. These are also isometric to $\widetilde{R_2}$ and $\widetilde{R_2^{-1}}$, by applying the isometry σ_{12}.

From $\widetilde{R_1 R_2}$ we can also deduce $\widetilde{(R_1 R_2)^{-1}}$, but this face is not isometric with $\widetilde{R_2 R_1}$, unless $t = 0$. It turns out that the combinatorics of $\widetilde{R_1 R_2}$ and $\widetilde{R_2 R_1}$ are the same only when $|t| \leq t_1$.

8.2. **Codimension two faces and cycles.** There are of course many isometries between the 2-faces, obtained by analyzing the cycles, in the terminology of the Poincaré polyhedron theorem (see section 7). Since we have introduced some new faces to the list given in [Mos80], we include a list of these cycles (valid only for small phase shift).

The face $\widetilde{R_i} \cap \widetilde{R_i^{-1}}$ is fixed by R_i since it is simply the mirror of that complex reflection. The cycle transformation is of course the reflection R_i, and it rotates complex hyperbolic space in the direction normal to its mirror by an angle $2\pi/p$. The copies of F_{12} under powers of R_i tile a neighborhood of that edge by construction, since the bisector $\widehat{R_i^{-1}}$ is obtained from $\widehat{R_i}$ by applying R_i. In the finite groups Γ_{ij}, no other pairs of elements yield cospinal bisectors.

The other cycles correspond to Giraud 2-faces. Recall that such an edge is contained in precisely three bisectors because of Giraud's theorem (see Theorem 4.9, and also the discussion in section 7), hence the corresponding cycles will have length three.

The cycles yield the following presentation for the finite group

$$\Gamma_{ij} = \langle R_i, R_j \mid R_i^p,\ R_iR_jR_i = R_jR_iR_j \rangle$$

Indeed the relation stating that R_i has order p comes from the 2-face on the mirror of R_i, and the braid relation is deduced from certain Giraud 2-faces. For instance, the fourth diagram below implies that the cycle transformation for the edge $\widetilde{R_2^{-1}} \cap \widetilde{(R_1R_2R_1)^{-1}}$ is given by

$$(R_1R_2R_1)(R_1R_2)^{-1}R_2^{-1}$$

This transformation is the identity because it fixes a Giraud disk, so we get

$$R_1R_2R_1 = R_2R_1R_2$$

One verifies that all relations obtained from the cycles below are trivial, except for the second and fourth cycles in the list below (both yield a relation equivalent to the braid relation).

The following four cycles correspond to triangular faces with one vertex at p_{12} (having the same combinatorics as in Figure 4). The first two consist of isometric 2-faces, and so do the last two, but the first and third are not isometric (unless $t = 0$).

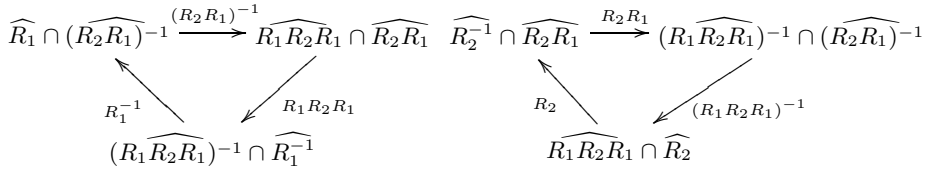

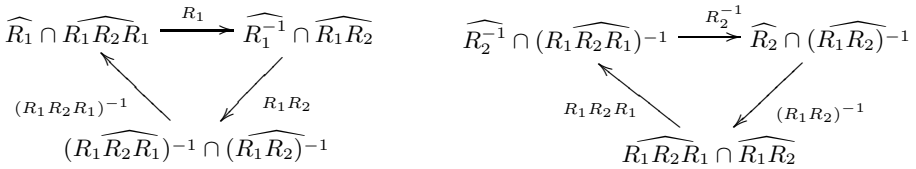

The following four cycles correpond to faces that do not contain p_{12}, and have the same combinatorics as in Figure 5. Once again there are two isometry types among them unless $t = 0$.

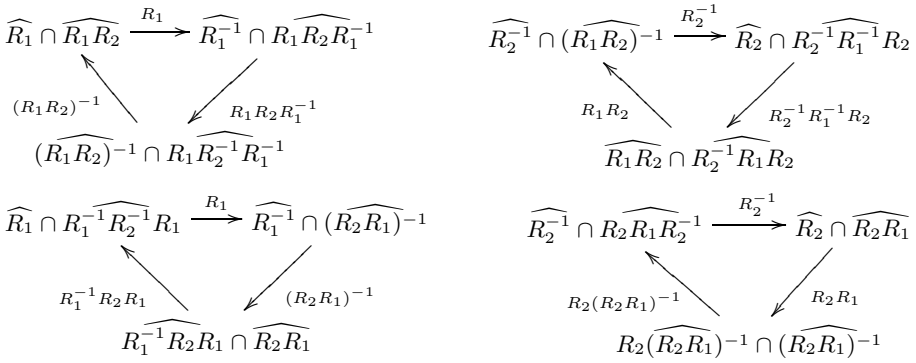

The following six cycles come in isometric pairs. They have one vertex and two (non geodesic) edges that go off to the boundary.

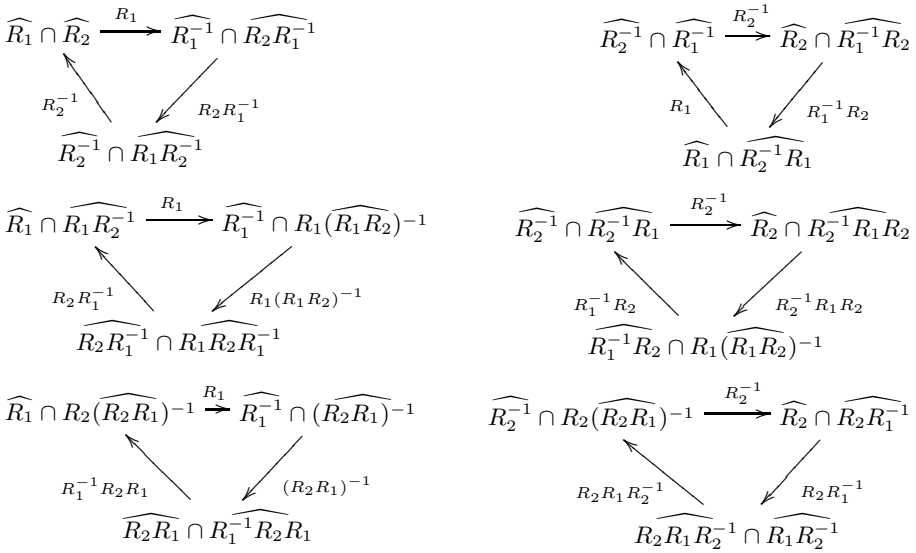

The 2-faces in the last two cycles have three vertices (one of which is p_{12}). They are not isometric unless $t = 0$.

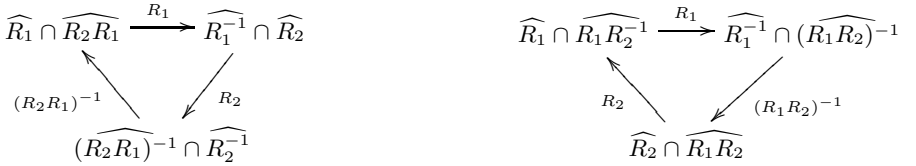

9. List of the main vertices

We now give the useful list of formulas for the vertices of the fundamental domain that appear in [Mos80]. As we shall discuss in section 11, in some cases there are extra vertices (this happens only for $p = 5$ and large phase shift).

For large phase shift, our notation differs slightly from [Mos80]: we have chosen to keep the same notation for the vertices for arbitrary phase shift, whereas Mostow describes the vertices s_{ij} by two different formulas (compare with Lemma 12.3 in [Mos80]). This should not cause any confusion, since the formulas given below define the points unambiguously, for arbitrary phase shift).

$$\begin{aligned} p_{12} &= [\xi, \overline{\xi}, 1-\alpha^2]^T \\ p_{23} &= Jp_{12} = [1-\alpha^2, \xi, \overline{\xi}]^T \\ p_{31} &= Jp_{23} = [\overline{\xi}, 1-\alpha^2, \xi]^T \end{aligned}$$

where $\xi = \alpha\varphi(1 + \alpha\overline{\varphi}^3)$.

$$\begin{aligned} s_{12} &= [\overline{\eta}i\varphi, \overline{\eta}i\overline{\varphi}, 1]^T \\ s_{23} &= Js_{12} = [1, \overline{\eta}i\varphi, \overline{\eta}i\overline{\varphi}]^T \\ s_{31} &= Js_{23} = [\overline{\eta}i\overline{\varphi}, 1, \overline{\eta}i\varphi]^T \end{aligned}$$

$$\begin{aligned} \tilde{s}_{21} &= [-\eta i\varphi, -\eta i\overline{\varphi}, 1]^T \\ \tilde{s}_{32} &= J\tilde{s}_{21} = [1, -\eta i\varphi, -\eta i\overline{\varphi}]^T \\ \tilde{s}_{13} &= J\tilde{s}_{32} = [-\eta i\overline{\varphi}, 1, -\eta i\varphi]^T \end{aligned}$$

$$\begin{aligned} t_{12} &= [a(\overline{\varphi}), \overline{a(\overline{\varphi})}, \alpha|a(\overline{\varphi})|^2]^T \\ t_{21} &= [\overline{a(\varphi)}, a(\varphi), \alpha|a(\varphi)|^2]^T \\ t_{23} &= Jt_{12} = [\alpha|a(\overline{\varphi})|^2, a(\overline{\varphi}), \overline{a(\overline{\varphi})}]^T \\ t_{32} &= Jt_{21} = [\alpha|a(\varphi)|^2, \overline{a(\varphi)}, a(\varphi)]^T \\ t_{31} &= Jt_{23} = [\overline{a(\overline{\varphi})}, \alpha|a(\overline{\varphi})|^2, a(\overline{\varphi})]^T \\ t_{13} &= Jt_{32} = [a(\varphi), \alpha|a(\varphi)|^2, \overline{a(\varphi)}]^T \end{aligned}$$

where $a(x) = \overline{x}(1 - \eta i x^3)$.

$$\begin{aligned} v_{123} &= [-\eta i\overline{\varphi}, 1, \overline{\eta} i\varphi]^T \\ v_{231} &= [\overline{\eta} i\varphi, -\eta i\overline{\varphi}, 1]^T \\ v_{312} &= [1, \overline{\eta} i\varphi, -\eta i\overline{\varphi}]^T \\ v_{321} &= [\overline{\eta} i\overline{\varphi}, 1, -\eta i\varphi]^T \\ v_{132} &= [-\eta i\varphi, \overline{\eta} i\overline{\varphi}, 1]^T \\ v_{213} &= [1, -\eta i\varphi, \overline{\eta} i\overline{\varphi}]^T \end{aligned}$$

For small phase shift (i.e. $|t| < 1/2 - 1/p$), the fundamental domain for the finite group Γ_{12} has 11 vertices, given by the p_{12}, s_{ij}, $\tilde{s}_{ij}$, t_{13}, t_{31}, t_{23}, t_{32}. When the hypotheses of the Poincaré theorem hold, the fundamental domain for Γ is the intersection of the three fundamental domains for the finite groups Γ_{ij} and has 15 vertices given by the first fifteen of the above formulas.

The following formulas are quite useful, as they give a partial explanation of the change of behavior in the fundamental domains for the groups as the phase shift is increased beyond its critical value, namely $|t| = \frac{1}{2} - \frac{1}{p}$.

$$\langle s_{12}, s_{12}\rangle = 1 - \frac{\cos(\pi t)}{\sin(\frac{\pi}{p})} \tag{9.1}$$

$$\langle v_{312}, v_{312}\rangle = 1 + \frac{\cos(\frac{2\pi}{p} - \pi t)}{\sin(\frac{\pi}{p})} \tag{9.2}$$

$$\langle v_{321}, v_{321}\rangle = 1 + \frac{\cos(\frac{2\pi}{p} + \pi t)}{\sin(\frac{\pi}{p})} \tag{9.3}$$

One checks directly that s_{12} is a negative vector if and only if $|t| < \frac{1}{2} - \frac{1}{p}$, v_{312} is negative for $t < -(\frac{1}{2} - \frac{1}{p})$, and v_{321} is negative for $t > \frac{1}{2} - \frac{1}{p}$ (see [Mos80], p. 228).

For completeness we mention that

$$\langle t_{32}, t_{32}\rangle = 2\left(1 - \cos(\frac{\pi}{p} + \frac{\pi}{2} + \pi t)\right)\left\{1 - \frac{\sin^2(\frac{\pi}{2p} + \frac{\pi}{4} + \frac{\pi}{2}t)}{\sin^2(\frac{\pi}{p})}\right\} \tag{9.4}$$

This implies that t_{32} is a negative vector if and only if $t > -(\frac{1}{2} - \frac{1}{p})$. Similarly, t_{23} is negative if and only if $t < \frac{1}{2} - \frac{1}{p}$.

10. The Picard integrality conditions

In this section we review how the cycles of 2-faces of the Dirichlet domains yield the integrality conditions in Theorem 2.7. These are

sometimes called the Picard integrality conditions (they appear already in [Pic81]).

Strictly speaking, the results of this section are valid only for $p = 3$ and 4, since for $p = 5$ the Dirichlet domain has additional faces (see section 11). Note however that the analysis of the cycles for complex geodesic 2-faces remains the same for $p = 5$, and all differences arise from generic 2-faces only (for which the only discreteness condition is that W be Giraud-closed, see section 7).

The figures of this section are included mainly for completeness, most of them being already in [Mos80] (except for Figure 8(d), which turns out to be crucial in [DFP05]). There are several difficulties about proving the results, but the numerical methods above give an easy way to test the claims experimentally.

Remark 10.1. The Dirichlet domains for the group $\Gamma = \Gamma(p, t)$ turn out to be the intersection of the Dirichlet domains for the three finite groups Γ_{ij} generated by any two of the three generators

$$F = F_{12} \cap F_{23} \cap F_{31}$$

We have seen in section 6 that the Dirichlet domains for the finite groups have many more faces than was stated in [Mos80], and it is perhaps surprising that the domains for the full lattices end up differing very little from Mostow's. This is explained by the fact that many of the extra faces for the finite groups are far from the fixed point of the corresponding finite group (see Figures 6 and 7).

Since the group G generated by the reflections R_i together with the symmetry J is slightly more natural than Γ itself, we describe a fundamental domain F_G for G. This involves decomposing the domain F into three cells, images under J of one another. A natural fundamental domain for the action of J is the sector in complex hyperbolic space bounded by two bisectors $B_1 = B(p_{12}, p_{13})$ and $B_2 = B(p_{12}, p_{23})$. Their complex spines are given by the mirrors of R_1 and R_2 respectively.

Some of the faces of the resulting polyhedron are illustrated in Figure 8, whose pictures are drawn in coordinates adapted to each bisector, i.e. so that the spine is along the vertical axis, horizontal planes correspond to complex slices and vertical planes containing the vertical axis yield the meridians. The polyhedron has a total of 12 faces, lying on the bisectors

$$R_1^{\pm 1}, R_2^{\pm 1}, (R_1R_2)^{\pm 1}, (R_2R_1)^{\pm 1}, (R_1R_2R_1)^{\pm 1}, B_1, B_2 \tag{10.1}$$

The side pairings are of course given by

$$\begin{aligned} R_1 &: \widehat{R_1} \to \widehat{R_1^{-1}} \\ R_2 &: \widehat{R_2} \to \widehat{R_2^{-1}} \\ R_1R_2 &: \widehat{R_1R_2} \to (\widehat{R_1R_2})^{-1} \\ R_2R_1 &: \widehat{R_2R_1} \to (\widehat{R_2R_1})^{-1} \\ R_1R_2R_1 &: \widehat{R_1R_2R_1} \to (R_1\widehat{R_2R_1})^{-1} \\ J &: B_1 \to B_2 \end{aligned}$$

There are three types of totally geodesic 2-faces, namely triangles contained in the mirrors of the R_j (the bottom face in Figure 8(a)), and triangles contained in slices of the bisectors $\widehat{R_1R_2}$ and $\widehat{R_2R_1}$ (the top and bottom faces in Figure 8(d)).

The cycle transformation fixing the mirror of R_j is of course simply R_j, and this trivially satisfies the conditions of the Poincaré theorem, since R_j rotates by an angle of $2\pi/p$ in the normal direction (see also the discussion in section 8).

We now consider the cycles for the geodesic face $\widehat{R_1R_2} \cap B_1 \cap F_G$. The discussion below is valid for $t > -(\frac{1}{2} - \frac{1}{p})$ (otherwise there is no such 2-face in the fundamental domain).

Lemma 10.2. *$\widetilde{R_1R_2} \cap B_1$ is a geodesic triangle on a complex geodesic that is the slice through t_{32} of any of the three bisectors $\widehat{R_1R_2}$, B_1 and $(\widehat{R_3R_1})^{-1}$ (that complex geodesic can also be described as $v_{312}^{\perp}$).*

Proof: One checks explicitly that $J^{-1}R_1R_2 = R_3R_1J^{-1}$ is a complex reflection with mirror $v_{312}^{\perp}$. Its mirror is by definition contained in $J^{-1}\widehat{R_1R_2} = \widehat{R_1R_2}$ and in $J(\widehat{R_3R_1})^{-1} = (\widehat{R_3R_1})^{-1}$. The last two equalities follow from the fact that p_0 is fixed by J.

One verifies directly that v_{312} is on the extended real spine of B_1, specifically

$$p_{31} + \eta i\varphi p_{12} = \alpha^2(\eta^2\varphi^2 + \eta i\varphi)v_{312} \tag{10.2}$$

so that $v_{312}^{\perp}$ is indeed also a slice of B_1. The fact that t_{32} is on the relevant complex geodesic follows from verifying directly that $\langle t_{32}, v_{312}\rangle = 0$, using the formulas from section 9. □

Lemma 10.3. *R_1R_2 maps $\widetilde{R_1R_2} \cap B_1$ to $(\widetilde{R_1R_2})^{-1} \cap B_2$. The cycle transformation for the edge $\widetilde{R_1R_2} \cap B_1$ is $J^{-1}R_1R_2$.*

Proof: One verifies by direct calculation that R_1R_2 maps t_{32} to t_{13}. It follows that it maps the slice of $\widehat{R_1R_2}$ through t_{32} to the slice of $(\widehat{R_1R_2})^{-1}$ through t_{13}, which are precisely the complex lines that appear in the lemma. □

Lemma 10.3 gives a natural necessary condition for F_W to be a fundamental domain, by examining the angle of rotation of the reflection $J^{-1}R_1R_2$.

Lemma 10.4. *The reflection $J^{-1}R_1R_2$ rotates by an angle $2\pi(\frac{1}{4}-\frac{1}{2p}+\frac{t}{2})$ about its mirror, and maps $\widehat{R_1R_2}$ to $(\widehat{R_3R_1})^{-1}$.*

This is done by a direct calculation (computing the eigenvalues of that matrix, and multiplying by the appropriate scalar matrix to give it the form (2.3)). The statement about sending one bisector to the other follows from Lemma 10.3, and the fact that J^{-1} maps $(\widehat{R_1R_2})^{-1}$ to $(\widehat{R_3R_1})^{-1}$.

In order for the conditions of the Poincaré polyhedron theorem, one requires the angle in Lemma 10.4 to be of the form π/k for some integer $k \in \mathbb{Z}$ (see section 7). This gives one of the integrality conditions in Theorem 2.7.

The second integrality condition comes from the analysis of the cycle transformation for the face $\widetilde{R_2R_1}\cap B_2$ (there is such a face in the domain only if $t < (\frac{1}{2}-\frac{1}{p})$). One verifies that this cycle transformation is given by the complex reflection R_2R_1J, and that it rotates about its mirror by an angle $2\pi(\frac{1}{4}-\frac{1}{2p}-\frac{t}{2})$.

Finally we mention that from the above analysis, one obtains a presentation for the Mostow lattices, by following the various cycles and cycle transformations. The relations are given in Table 2, where we only list some 2-faces (the relations coming from other faces are all consequences of the ones given in the table). Here we write k and l for the integers that appear in Theorem 2.7, namely

$$\begin{aligned} \tfrac{1}{4}-\tfrac{1}{2p}+\tfrac{t}{2} &= \tfrac{1}{k} \\ \tfrac{1}{4}-\tfrac{1}{2p}-\tfrac{t}{2} &= \tfrac{1}{l} \end{aligned} \tag{10.3}$$

11. Varying the parameters

As was mentioned above, it is quite difficult to analyze how the combinatorics of the Dirichlet domains change as the parameters p and t vary. We now summarize the results of our experimental observations, and show that some modifications are needed in the domains described in [Mos80].

2-face	relation	type
$\widehat{R_i \cap R_i^{-1}}$	$R_i^p = 1$	complex
$\widehat{R_2 \cap R_1 R_2 R_1}$	$R_1R_2R_1 = R_2R_1R_2$	generic
$\widehat{B_1 \cap B_2}$	$J^3 = 1$	generic
$\widehat{R_1R_2 \cap B_1}$	$(J^{-1}R_1R_2)^k = 1$	complex
$\widehat{R_2R_1 \cap B_2}$	$(R_2R_1J)^l = 1$	complex

TABLE 2. The relations obtained from the cycles of 2-faces. The integers k and l are defined by (10.3).

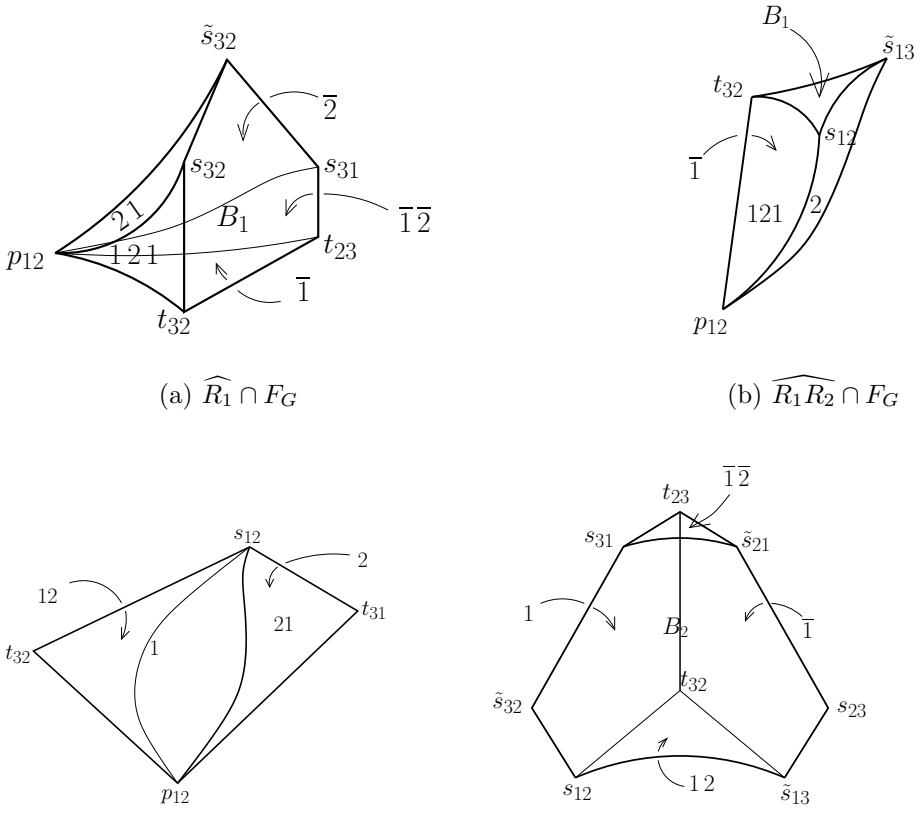

(a) $\widehat{R_1} \cap F_G$

(b) $\widehat{R_1R_2} \cap F_G$

(c) $\widehat{R_1R_2R_1} \cap F_G$

(d) $B_1 \cap F_G$

FIGURE 8. The combinatorics of some faces of the fundamental domain F_G for G, for $p = 3$ and small phase shift ($t = 1/12$).

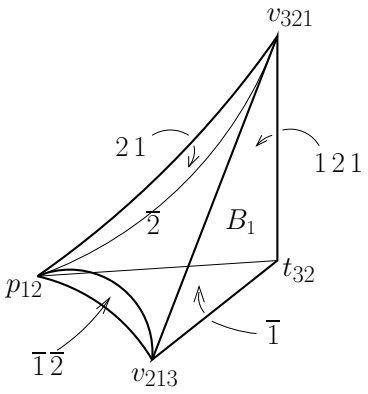

(a) $\widehat{R_1} \cap F_G$

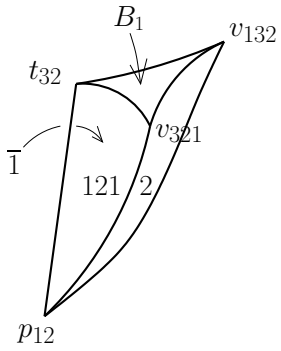

(b) $\widehat{R_1R_2} \cap F_G$

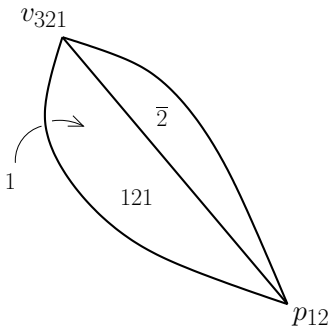

(c) $\widehat{R_2R_1} \cap F_G$

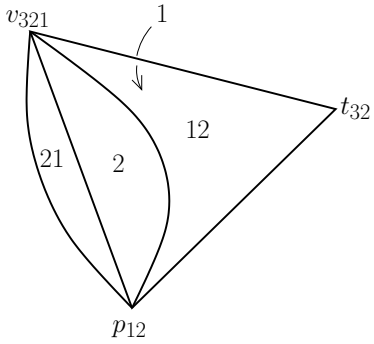

(d) $\widehat{R_1R_2R_1} \cap F_G$

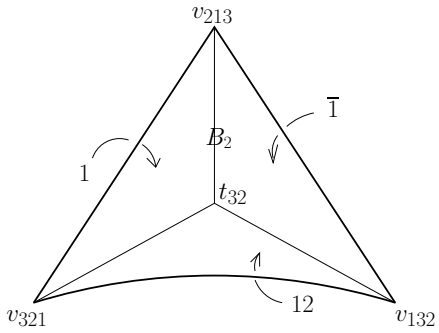

(e) $B_1 \cap F_G$

FIGURE 9. The combinatorics of some faces of the fundamental domain F_G for G, for $p = 3$ and large phase shift ($t = 1/3$). Note that we write $i, \overline{i}$ for R_i, R_i^{-1}, respectively.

11.1. **Summary of experimental observations.** We shall write

$$W_M = \{R_i^{\pm 1}, (R_iR_j)^{\pm 1}, (R_iR_jR_i)^{\pm 1}\} \tag{11.1}$$

for the set of words that appears in [Mos80]. Our experimental observations suggest the following:

(1) For any p and small phase shift, i.e. $|t| \leq \frac{1}{2} - \frac{1}{p}$, $F = F_W$ for $W = W_M$ and Mostow's combinatorics are correct.
(2) For $p < 5$ and large phase shift, i.e. $|t| > \frac{1}{2} - \frac{1}{p}$, $F = F_W$ for $W = W_M$, with combinatorics described in Figure 9.
(3) For $p = 5$ and large phase shift, $F = F_W$ for
$$W = W_M \cup \{(R_iR_j)^{\pm 2}\}$$
with different combinatorics for the two relevant values of t (see Figure 12 and 13).

We do not state the preceding results as a theorem, since in principle it is conceivable that more faces be discovered by using a more precise computer program (in the same way that we have found errors in Mostow's analysis by using much more sophisticated computers).

We emphasize the fact that the Dirichlet domains for the groups $\Gamma(5, 11/30)$ and $\Gamma(5, 7/10)$ do not have the same combinatorics, even though they both correspond to large phase shift. This differs once again with the analysis given in [Mos80], and in particular one needs to be extremely cautious about the behavior of Dirichlet polyhedra as parameters vary.

In fact, our experimental methods apply to study the combinatorics of F_W only for a fixed value of t, and we shall not attempt to study the stability of the combinatorics as t varies. This is not a big restriction if we want to study the finite number of lattices that arise from this construction (we focus only on the values in Table 1). Note however that in order to use these methods for polyhedra corresponding to non-discrete groups (to contruct non-locally symmetric Kähler manifolds as in [MS80]), one would have to study this stability question more carefully (in fact for that purpose, it is more convenient to use the algebro-geometric description of those groups as monodromy groups of hypergeometric functions, see [Der04] for instance).

When the group satisfies the conditions for discreteness, the Dirichlet polyhedron is only "almost" a fundamental domain for the full group Γ generated by R_1, R_2 and R_3, since in many cases the center p_0 is fixed by non-trivial elements in the group. It can be checked that the stabilizer of p_0 is finite, and that it is either trivial or cyclic of order three, generated by the transformation J (which often turns out to be in the group generated by the reflections R_i).

11.2. **The case $p = 5$, for large phase shift.** In this section we describe the combinatorics of the Dirichlet domains for $\Gamma(5, t)$, $t > 3/10$ (a similar analysis holds for $t < -3/10$). Our domains are "slightly smaller" than the ones described in [Mos80], in the sense that we include a few more bisectors to define the Dirichlet polyhedra.

It turns out that the Dirichlet domains for the two discrete groups with large phase shift ($t = 11/30$ and $7/10$) have significantly different combinatorics (see Figures 12 and 13). In particular, contrary to what was stated in [Mos80], the combinatorics are not independent of p, and there are more cases than simply small and large phase shift.

We describe one specific place where the analysis in [Mos80] breaks down for the above two groups, and analyze the polyhedron F_W, where W is as in (11.1), namely

$$W = \{R_i^{\pm 1}, (R_i R_j)^{\pm 1}, (R_i R_j R_i)^{\pm 1}\} \tag{11.2}$$

The error can be seen by experimentation, exploring the combinatorics of 2-face $F_W \cap \widehat{R_1} \cap \widehat{R_2^{-1}}$. For small phase shift, it is bounded by $\widehat{R_3 R_1}$, $\widehat{R_2 R_1}$ and $(\widehat{R_2 R_1})^{-1}$, the last two intersecting in p_{12} (it is obvious that p_{12} is contained in these bisectors, since it is by definition fixed by both R_1 and R_2). It turns out more bisectors enter the picture for large phase shift.

Let c_{21} (resp. c_{121}) be the curve $\widehat{R_1} \cap \widehat{R_2^{-1}} \cap \widehat{R_2 R_1}$ (resp $\widehat{R_1} \cap \widehat{R_2^{-1}} \cap \widehat{R_1 R_2 R_1}$). We shall not prove the following experimental observations, but urge the reader to test the claims for themselves, for instance by using the Java application [Der] (see Remark 4.13 about notation).

Proposition 11.1. *(1) The curves c_{21} and c_{121} intersect at p_{12} and they are tangent at that point precisely when $t = 3/10$.*

(2) For small phase shift, their intersection contains precisely one other point q_{12}, approaching p_{12} as t approaches $3/10$.

(3) For $t = 3/10$, the curves intersect in the boundary of complex hyperbolic space.

(4) For large phase shift, the curves intersect in three points (in the ball) – we still denote by q_{12} the one that is closest to p_{12}. The point q_{12} is a vertex of F_W.

Remark 11.2. (1) Similar conclusions hold for the curves corresponding to $(R_2 R_1)^{-1}$ and $(R_1 R_2 R_1)^{-1}$. If $t = -3/10$, a similar statement is true for some other 2-face of F_W, corresponding to R_1^{-1} and R_2.

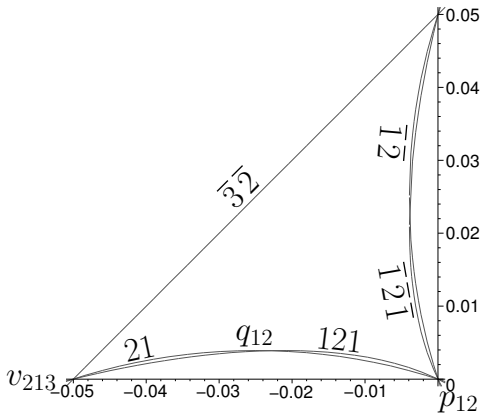

FIGURE 10. The 2-face $F_W \cap \widehat{R_1} \cap \widehat{R_2^{-1}}$, for $p = 5$ and large phase shift ($t = 6/10$).

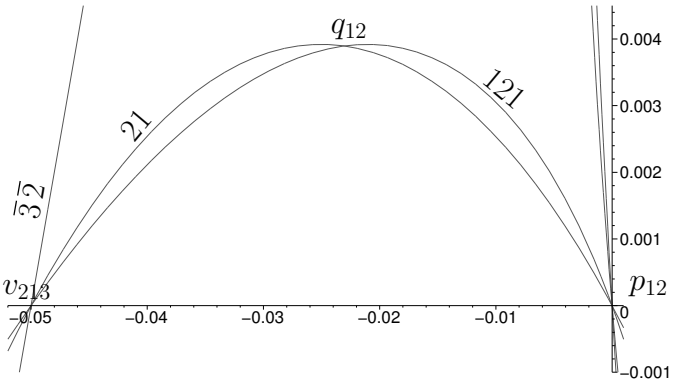

FIGURE 11. Zoomed version of Figure 10.

(2) The point q_{12} turns out to be a vertex of the fundamental domain for $t = 11/30$. When $t = 7/10$, it coincides with v_{213}, where the two curves are again tangent.
(3) The curves c_{21} and c_{121} are very close to each other, and in fact barely distinguishable near p_{12} (see Figures 10 and 11)

We now state some consequences of the above changes in the combinatorics of F_W as t goes through critical phase shift (the most concrete formulation being part 2 of the proposition).

Proposition 11.3. *Let $p = 5$ and $t > 3/10$.*

(1) The polyhedron F_W has a nonempty face on the bisector intersection $\widehat{R_1} \cap (\widehat{R_1 R_2 R_1})^{-1}$.

(2) R_1 maps $\widehat{R_1} \cap (\widehat{R_1R_2R_1})^{-1}$ to $\widehat{R_1^{-1}} \cap (\widehat{R_1R_2})^{-2}$, and the polyhedron F_W, where W is as in (11.2), does not have side pairings.

Remark 11.4. Part 1 of the proposition can be interpreted as exhibiting some extra intersections between the faces of F_W, omitted in the description from [Mos80]. Note also that both claims in the proposition hold only for $p = 5$. For $p = 3$ or 4, Mostow's polyhedra seem to be correct.

Proof: Note that (2) follows from (1) together with Giraud's theorem. Indeed, R_1 maps this bisector intersection to $\widehat{R_1} \cap \widehat{\gamma}$ where

$$\gamma = (R_1R_2R_1)^{-1}R_1^{-1} = (R_2R_1R_2)^{-1} \cdot R_1^{-1} = (R_1R_2)^{-2}$$

as follows from (4.4). The latter intersection is contained in precisely three bisectors, only two of which are equidistant from p_0 (cf. Theorem 4.9).

We claim that $(\widehat{R_1R_2})^{-2}$ is not among the list of bisectors $\widehat{w}$, $w \in W$. Rather than proving this for general phase shift, we simply mention that, for any fixed value of the phase shift, this claim amounts to verifying that none of twenty four group elements fixes p_0 (namely the elements $(R_1R_2)^2w$, $w \in W$). For $p = 5$ and large phase shift there are two relevant values, $|t| = 11/30$ and $|t| = 7/10$.

Now part (1) can be checked numerically. For instance, consider the case $t = 11/30$. We claim that the point z on $\widehat{R_1} \cap (\widehat{R_1R_2R_1})^{-1}$ with spinal coordinates $u_j = e^{2\pi i t_j}$ where $t_1 = -0.0011$ and $t_2 = 0.0075$ is in the interior of this 2-face of F_W. This follows from verifying 22 inequalities of the form

$$|\langle z, p_0\rangle| < |\langle z, w^{-1}p_0\rangle|$$

where $w \in W$ is different from R_1 and $(R_1R_2R_1)^{-1}$ (note that W has 24 elements). This can easily be done with the computer. □

The proof also suggests an extra set of words that need to be included in order to have side pairings, namely the $(R_iR_j)^{\pm 2}$ (see the discussion at the end of section 7). Experimentation suggests that in both cases $\Gamma(5, 11/30)$ and $\Gamma(5, 7/10)$ no other words need to be included (i.e. that the corresponding set of words is Giraud-closed). However, this depends on combinatorics that are obtained experimentally, and it is conceivable that a more precise computation would yield extra intersections between the various relevant bisectors, forcing us to introduce yet another set of words in order for the polyhedron to have side pairings.

The conjectural combinatorics are summarized in Figures 12 and 13.

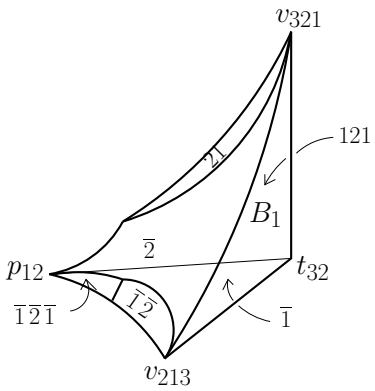

(a) $\widehat{R_1} \cap F_G$

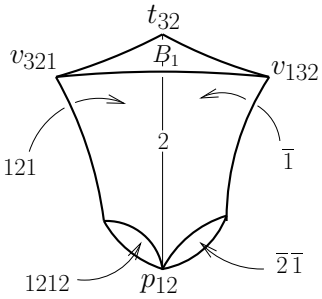

(b) $\widehat{R_1R_2} \cap F_G$

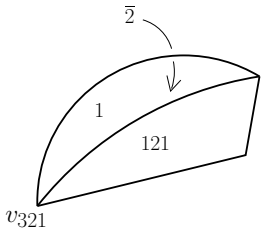

(c) $\widehat{R_2R_1} \cap F_G$

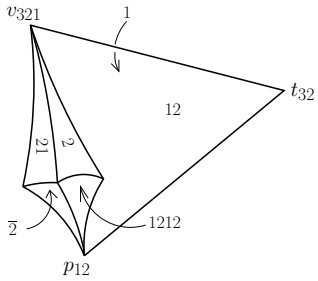

(d) $\widehat{R_1R_2R_1} \cap F_G$

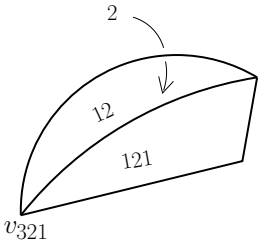

(e) $(\widehat{R_1R_2})^2 \cap F_G$

FIGURE 12. Combinatorics of the fundamental domain, for $p = 5$ and $t = 11/30$.

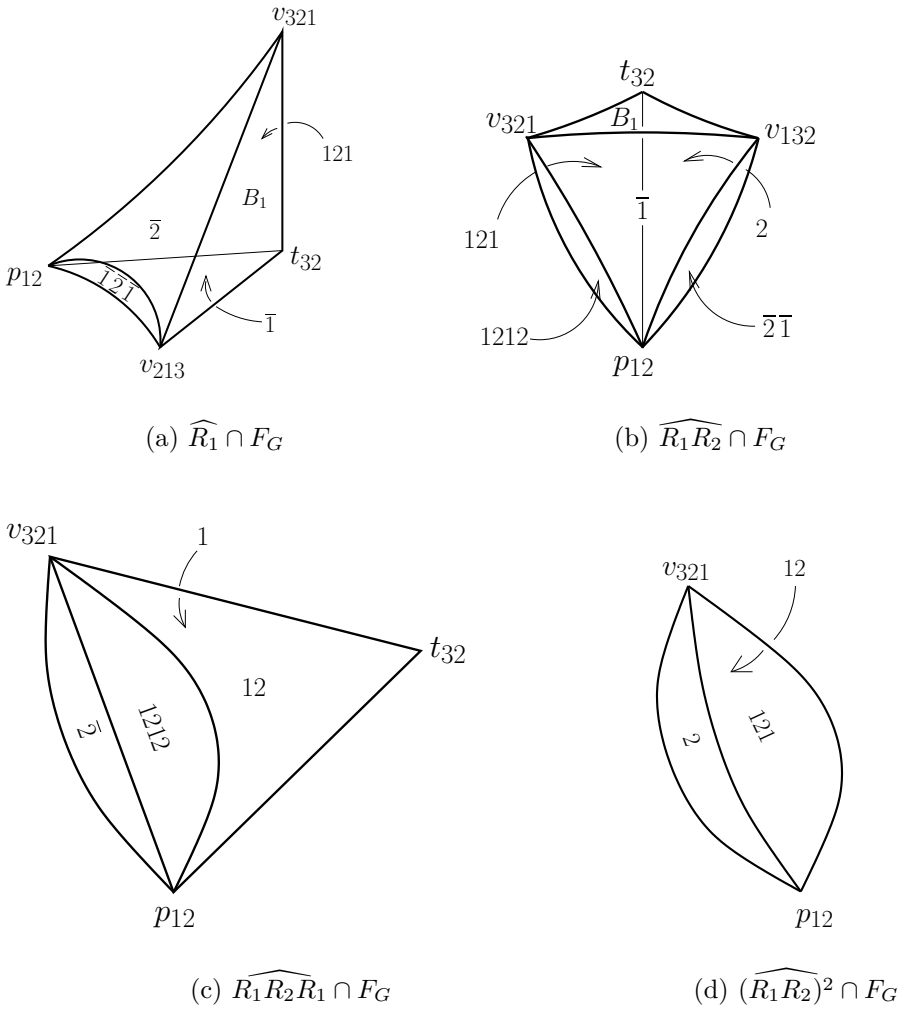

(a) $\widehat{R_1} \cap F_G$ (b) $\widehat{R_1R_2} \cap F_G$

(c) $\widehat{R_1R_2R_1} \cap F_G$ (d) $(\widehat{R_1R_2})^2 \cap F_G$

FIGURE 13. Combinatorics of the fundamental domain, for $p = 5$ and $t = 7/10$. In this case $\widehat{R_2R_3} = (\widehat{R_3R_1})^{-1}$.

REFERENCES

[Cox67] H. S. M. Coxeter. Finite groups generated by unitary reflections. *Abh. Math. Sem. Univ. Hamburg*, 31:125–135, 1967.

[Der] M. Deraux. Dirichlet polyhedra for the Mostow lattices. Java applet, `http://www.math.utah.edu/~deraux/java/mostow`.

[Der04] M. Deraux. On the universal cover of certain exotic Kähler surfaces of negative curvature. *Math. Ann.*, 329(4):653–683, 2004.

[Der05] M. Deraux. Deforming the $\mathbb{R}$-Fuchsian (4,4,4)-triangle group into a lattice. preprint, 2005.

[DFP05] M. Deraux, E. Falbel, and J. Paupert. New constructions of fundamental polyhedra in complex hyperbolic space,. To appear in Acta Math., 2005.

[DM86] P. Deligne and G. D. Mostow. Monodromy of hypergeometric functions and non-lattice integral monodromy. *Inst. Hautes Études Sci. Publ. Math.*, 63:5–89, 1986.

[Eps87] D. B. A. Epstein. Complex hyperbolic geometry. In *Analytical and Geometric Aspects of Hyperbolic Space*, volume 111 of *London Math. Soc. Lecture Notes*, pages 93–111. Cambridge University Press, Cambridge, 1987.

[FK02] E. Falbel and P.-V. Koseleff. Rigidity and flexibility of triangle groups in complex hyperbolic geometry. *Topology*, 41(4):767–786, 2002.

[FP04] E. Falbel and J. Paupert. Fundamental domains for finite subgroups of U(2) and configurations of lagrangians. *Geom. Dedicata*, 109:221–238, 2004.

[FP05] E. Falbel and J. Parker. The geometry of the Eisenstein-Picard modular group. to appear in Duke Math. J., 2005.

[Gir21] G. Giraud. Sur certaines fonctions automorphes de deux variables. *Ann. Sci. École Norm. Sup.*, 38:43–164, 1921.

[Gol99] W. M. Goldman. *Complex Hyperbolic Geometry*. Oxford Mathematical monographs. Oxford University Press, 1999.

[GP92] W. M. Goldman and J. R. Parker. Dirichlet polyhedra for dihedral groups acting on complex hyperbolic space. *J. Geom. Anal.*, 2(6):517–554, 1992.

[Mos80] G. D. Mostow. On a remarkable class of polyhedra in complex hyperbolic space. *Pacific J. Math.*, 86:171–276, 1980.

[Mos86] G. D. Mostow. Generalized Picard lattices arising from half-integral conditions. *Inst. Hautes Études Sci. Publ. Math.*, 63:91–106, 1986.

[Mos88] G. D. Mostow. On discontinuous action of monodromy groups on the complex n-ball. *J. Amer. Math. Soc.*, 1:555–586, 1988.

[MS80] G. D. Mostow and Y. T. Siu. A compact Kähler surface of negative curvature not covered by the ball. *Ann. of Math.*, 112:321–360, 1980.

[Par05] J. Parker. Cone metrics on the sphere and Livne's lattices. Preprint, 2005.

[Phi92] M. Phillips. Dirichlet polyhedra for cyclic groups in complex hyperbolic space. *Proc. Amer. Math. Soc.*, 115:221–228, 1992.

[Pic81] E. Picard. Sur une extension aux fonctions de deux variables du problème de Riemann relatif aux fonctions hypergéométriques. *Ann. ENS*, 10:305–322, 1881.

[Sch01] R. E. Schwartz. Ideal triangle groups, dented tori, and numerical analysis. *Annals of Mathematics*, 153:533–598, 2001.

[Thu98] W. P. Thurston. Shapes of polyhedra and triangulations of the sphere. *Geometry and Topology Monographs*, 1:511–549, 1998.

Université de Grenoble, Institut Fourier, B.P. 74, 38402 Saint-Martin-d'Hères Cedex, France.

E-mail address: deraux@ujf-grenoble.fr